European Master in Biological and Chemical Engineering for a Sustainable Bioeconomy

Bioceb
European Master in Biological and Chemical Engineering for a Sustainable Bioeconomy

AgroParisTech

université PARIS-SACLAY

UNIVERSITÉ DE REIMS CHAMPAGNE-ARDENNE

TALTECH

A! Aalto University

LIÈGE université

Erasmus Mundus

Erasmus+

Master thesis report

submitted to obtain the degrees of

Master in Biology AgroSciences (BAS) of the University of Reims Champagne-Ardenne

Master of Science in Engineering of Tallinn University of Technology

Master of Science (Technology) of Aalto University

Developing applications for biorefinery lignin: chemical modification and nanoparticle preparation

Presented by: *GARCIA, Elijah Mark*

Defended the: 07/07/2023

Supervised by: **Österberg, Monika; Nousiainen, Paula; Farooq, Muhammad**

at: **Aalto University**

from: 01/01/2023 to 31/05/2023

Bioceb supervisors**: Österberg, Monika (Aalto University); Tarasova, Elvira (Tallinn University of Technology)**

Confidentiality: Yes ☐ No ◼   Privacy expiration date: …/…/….

Master's Programme in Biological and Chemical Engineering for a Sustainable Bioeconomy

Developing applications for biorefinery lignin: chemical modification and nanoparticle preparation

Elijah Mark Garcia

Master's Thesis
2023

Aalto-yliopisto
Aalto-universitetet
Aalto University

Author Elijah Mark Garcia	
Title of thesis Developing applications for biorefinery lignin: chemical modification and nanoparticle preparation	
Programme Biological and Chemical Engineering for a Sustainable Bioeconomy	
Major Materials and Biopolymers	
Thesis supervisor Prof. Monika Österberg	
Thesis advisor(s) Dr. Paula Nousiainen, Dr. Muhammad Farooq	
Date 15.06.2023 **Number of pages** 59 **Language** ENG	

Abstract

The sustainability of emerging lignocellulosic biorefineries warrants the complete utilization of all its fractionation streams, including lignin. However, there are existing technological gaps in the downstream processes of biorefineries, hindering the effective valorization of lignin streams. This research presents valuable insights into the chemical modification of biorefinery lignin and its effect on the structure, material properties, and supramolecular assembly of lignin into nanoparticles. Technical lignin obtained from the Dawn Technology ™ process was fractionated, and the soluble fraction was esterified with lauroyl chloride at different molar ratios. Extensive characterization using spectroscopic, chromatographic, and thermal methods was conducted to analyze the properties of both unmodified lignin and the resulting lignin laurates. The esterified lignins exhibited increased molecular weights, lower hydroxyl group contents, and demonstrated melting behaviors. Solvent exchange method was used to prepare colloidal nanoparticles from unmodified lignin (LNPs) and lignin laurates (La-LNPs). Notably, La-LNPs exhibited larger particle sizes compared to LNPs. Furthermore, we evaluated the performance of these nanoparticle dispersions as stabilizers for olive oil-in-water Pickering emulsions. Remarkably, the LNPs prepared from unmodified lignin demonstrated superior emulsification performance.

Keywords biorefinery lignin, lignin esterification, lignin nanoparticles, lignin laurate, Pickering emulsions

![Aalto University logo](Aalto-yliopisto Aalto-universitetet Aalto University)

Autor Elijah Mark Garcia	

Lõputöö pealkiri Biorafineerimistehase ligniini rakenduste väljatöötamine: keemiline modifitseerimine ja nanoosakeste valmistamine

Programm Biological and Chemical Engineering for a Sustainable Bioeconomy

Major Materials and Biopolymers

Lõputöö juhendaja Prof. Monika Österberg

Lõputöö nõustaja Dr. Paula Nousiainen, Dr. Muhammad Farooq

Kuupäev 15.06.2023 **Lehtede arv** 59	**Kell** EST	

Abstraktne

Loodavate lignotselluloosa biorafineerimistehaste jätkusuutlikkus nõuab kõigi selle fraktsioneerimisvoogude, sealhulgas ligniini täielikku kasutamist. Siiski on biorafineerimistehaste järeltöötlemisprotsessides tehnoloogilisi lünki, mis takistavad ligniinivoogude tõhusat väärindamist. Käesolevas uurimuses esitatakse väärtuslikke teadmisi biojahutusse mineva ligniini keemilisest modifitseerimisest ja selle mõjust struktuurile, materjaliomadustele ja ligniini supramolekulaarsele kokkupanemisele nanoosakesteks. Dawn Technology ™ protsessist saadud tehniline ligniin fraktsioneeriti ja lahustuv fraktsioon esterdati lauroüülkloriidiga erinevates molaarsetes suhetes. Nii modifitseerimata ligniini kui ka saadud ligniinilauraatide omaduste analüüsimiseks viidi läbi ulatuslik iseloomustus, kasutades spektroskoopilisi, kromatograafilisi ja termilisi meetodeid. Esterdatud ligniinid näitasid suuremat molekulmassi, väiksemat hüdroksüülrühmade sisaldust ja näitasid sulamiskäitumist. Kolloidsete nanoosakeste valmistamiseks modifitseerimata ligniinist (LNP) ja ligniinilauraatidest (La-LNP) kasutati lahustivahetuse meetodit. La-LNP-del olid võrreldes LNP-dega suuremad osakeste suurused. Lisaks hindasime nende nanoosakeste dispersioonide toimivust stabiliseerijatena oliiviõli-vees Pickeringi emulsioonides. Tähelepanuväärselt näitasid modifitseerimata ligniinist valmistatud LNP-d paremat emulgeerimisvõimet.

Märksõna biorafineerimise ligniin, ligniini esterdamine, ligniini nanoosakesed, ligniinilauraat, Pickeringi emulsioonid

AUTHOR'S DECLARATION

Hereby I declare, that I have written this thesis independently.
No academic degree has been applied for based on this material. All works, major viewpoints and data of the other authors used in this thesis have been referenced.

15.06.2023

Author: Elijah Mark Garcia
          /signature /

Thesis is in accordance with terms and requirements

15.06.2023

Supervisor: Elvira Tarasova
          /signature/

Accepted for defence

"......."...................20… .

Chairman of theses defence commission: ....

          /name and signature/

Non-exclusive licence for reproduction and publication of a graduation thesis[1]

I, Elijah Mark Garcia,

1. grant Tallinn University of Technology free licence (non-exclusive licence) for my thesis Developing applications for biorefinery lignin: chemical modification and nanoparticle preparation,

supervised by Elvira Tarasova,

1.1 to be reproduced for the purposes of preservation and electronic publication of the graduation thesis, incl. to be entered in the digital collection of the library of Tallinn University of Technology until expiry of the term of copyright;

1.2 to be published via the web of Tallinn University of Technology, incl. to be entered in the digital collection of the library of Tallinn University of Technology until expiry of the term of copyright.

2. I am aware that the author also retains the rights specified in clause 1 of the non-   exclusive licence.

3. I confirm that granting the non-exclusive licence does not infringe other persons' intellectual property rights, the rights arising from the Personal Data Protection Act or rights arising from other legislation.

15.06.2023

---

[1] *The non-exclusive licence is not valid during the validity of access restriction indicated in the student's application for restriction on access to the graduation thesis that has been signed by the school's dean, except in case of the university's right to reproduce the thesis for preservation purposes only. If a graduation thesis is based on the joint creative activity of two or more persons and the co-author(s) has/have not granted, by the set deadline, the student defending his/her graduation thesis consent to reproduce and publish the graduation thesis in compliance with clauses 1.1 and 1.2 of the non-exclusive licence, the non-exclusive license shall not be valid for the period.*

TalTech Department of Materials and Environmental Technology
THESIS TASK

Student: Elijah Mark Garcia, 231096KVEM

Study programme, Bioceb (KVEM)

main speciality: Biopolymers

Supervisor(s): Senior Lecturer, Elvira Tarasova, +372 620 2906

Consultants: …………………………………………………………..(name, position)

………………………………………………………………………… (company, phone, e-mail)

Thesis topic:

(in English) *Developing applications for biorefinery lignin: chemical modification and nanoparticle preparation*

(in Estonian)*Biorafineerimistehase ligniini rakenduste väljatöötamine: keemiline modifitseerimine ja nanoosakeste valmistamine*

Thesis main objectives:

1. To synthesize and characterize Dawn lignin esterified with lauroyl chloride
2. To prepare and characterize nanoparticles from Dawn lignin and its esters
3. To investigate the ability of the nanoparticles to stabilize oil-in-water emulsions

Thesis tasks and time schedule:

No	Task description		Deadline
1.	I.	Fractionation of crude Dawn lignin	3 months
	II.	Esterification of Dawn lignin with varying molar ratios of lauroyl chloride	
	III.	Characterization of Dawn lignin and lignin laurates with FTIR, NMR, GPC, and DSC	
2.	I.	Preparation of lignin nanoparticles (LNPs)	1 month
	II.	Preparation of lignin laurate nanoparticles (La-LNPs)	
	III.	Characterization of LNPs and La-LNPs with DLS and SEM	
3.	I.	Comparison of emulsification performance of LNPs and La-LNPs	1 month
	II.	Preparation of Pickering emulsions at varying LNP loading	

Language: English **Deadline for submission of thesis:** 15.06.2023

Student: Elijah Mark Garcia ....…….......... 15.06.2023

/signature/

Supervisor: Elvira Tarasova ………………………. 15.06.2023

/signature/

Head of study programme: Jaan Kers 15.06.2023

/signature/

Terms of thesis closed defence and/or restricted access conditions to be formulated on the reverse side

Contents

Preface

When I attended one of my professor's talks before, I never fully understood what he meant by embracing humility as the way forward in this harsh world.

Entering this master's program, I had a mindset of self-reliance, believing that my skills would be enough to overcome any challenges I would face. I was determined to assert my space and stand my ground. However, this journey, including the writing of this thesis, has humbled me on several occasions. The classes in plant genetics and development made me realize how my understanding of biology was severely limited despite it being my favorite subject at some point in my life. Moreover, I know what cellulose is, but I never really bothered about the other more complex component, lignin. And little did I know that later on, I would be having moments of frustration when my lignin nanoparticles were not forming in the way they should.

The completion of this thesis would not be possible without the people who have extended their spaces for me. First of all, I am deeply grateful to Prof. Monika Österberg for entrusting me with this project and for sharing her extensive knowledge throughout the entire process. My sincere gratitude also goes to Paula and Farooq for their patience and guidance, especially whenever I come knocking at their doors asking for help with my experiments. I am also thankful to the Bioproduct Chemistry group for fostering a welcoming environment within the research group, where fruitful discussions took place. I am indebted to the friends I have made during my master's program who became my support system here in Europe: my Bioceb family and the friends I made in Tallinn and here at Aalto University. And of course, I thank my family and friends back in the Philippines for the love and support that endure long distances.

Now, it seems clearer to me what my professor said about the value of humility in scientific research and in the grander scheme of things. I would not have reached this point if I had not been humble enough to acknowledge my limitations, admit mistakes in my methods, and most importantly, recognize the strength in seeking help when the burdens of life become overwhelming. When we embrace our personal limitations and strive collectively towards the relentless pursuit of truth, we can push the boundaries of knowledge and contribute to creating a more just world.

Otaniemi, 15th of June, 2023

Elijah Mark Garcia

Symbols and abbreviations

Symbols

θ	Water contact angle
δ	Chemical shift in the NMR spectra
Δm	Weight increase per gram of lignin

Abbreviations

AL	Alkali lignin
ATR-FTIR	Attenuated total reflection Fourier transform infrared spectroscopy
CNF	Cellulose nanofibrils
D_h	Hydrodynamic diameter
DLS	Dynamic light scattering
DMF	*N,N*-dimethylformamide
DMSO	Dimethylsulfoxide
DS	Degree of substitution
DSC	Differential scanning calorimetry
EH	Enzymatic hydrolysis
EtOH	Ethanol
G	guaiacyl unit of lignin
GPC	Gel permeation chromatography
H	*p-H*ydroxyphenyl unit of lignin
HSQC	heteronuclear single quantum coherence
IS	Internal standard
La-Lignin	Lignin laurate
La-LNPs	Lignin laurate nanoparticles
LNPs	Lignin nanoparticles
NMR	Nuclear magnetic resonance
O/W	Oil-in-water
OH	Hydroxyl group
OS	Organosolv
P NMR	Phosphorus Nuclear Magnetic Resonance
PLL	Poly-L-lysine
S	syringyl unit of lignin
SEM	Scanning electron microscopy
SKL	Softwood Kraft lignin
T_g	Glass transition temperature
THF	Tetrahydrofuran
T_m	Melting point

1 Introduction

Lignin is a class of diverse aromatic polymers making up roughly one-third of the dry weight of most terrestrial plants (Ragauskas et al., 2014). Traditionally, it is considered a waste product of the pulp and paper industry, and it is typically burned for energy, neglecting its potential for high-value products (Sharma et al., 2021). With the rise of lignocellulosic biorefineries, a paradigm shift towards the co-production of carbohydrate and lignin streams is also emerging. Techno-economic analyses highlight the significant role of lignin valorization in ensuring the vitality of these industries (Bajwa et al., 2019).

However, the main challenge to the efficient utilization of lignin is its structural complexity and heterogeneity which could pose several issues including varying degrees of reactivity, inconsistent material properties, and need for sophisticated characterization (Constant et al., 2016; Meng et al., 2019; Ralph et al., 2004). These constraints are brought about by its inherently diverse chemical structure, which is altered further by the reactions it undergoes during pulping and isolation. Collective efforts in characterizing lignin from various sources and developing technologies to convert it into valuable products are necessary to realize its potential.

One of the issues that limit the application of unmodified lignin is its poor dispersibility and incompatibility with hydrophobic matrices (Luo et al., 2017). Therefore, it is typically modified chemically to overcome these processability issues. The most common method is by esterifying its hydroxyl groups to improve its solubility in organic solvents and compatibility with non-polar polymers (Duval & Lawoko, 2014). More recently, the conversion of lignin into lignin nanoparticles (LNPs) with well-defined morphology and tunable surface properties has also gained significant attention as it bypasses the limitations of lignin as a complex macromolecule (Schneider et al., 2021). This transformation expands its application window from bulk use, like adhesives and composites, to novel applications, such as drug delivery and biocatalysis (Österberg et al., 2020).

The primary aim of this thesis is to bridge existing technological gaps in downstream processes of biorefineries for the effective valorization of lignin streams. This study focuses on the technical lignin obtained from Dawn Technology™, which employs acid hydrolysis to convert second-generation feedstocks (non-food biomass) into industrial sugars and lignin. Chemical modification and nanoparticle preparation are

explored as valorization routes for this biorefinery lignin. In detail, the objectives of this thesis are:

1. To analyze the structure and properties of the soluble fraction, simply referred to as Dawn lignin in this report, before and after esterification with lauroyl chloride at varying molar ratios.
2. To evaluate the effect of esterification on the supramolecular assembly of Dawn lignin into colloidal nanoparticles.
3. To investigate the applicability of the nanoparticles as stabilizers for olive oil-in-water Pickering emulsions.

An overview of the research is illustrated in Figure 1.
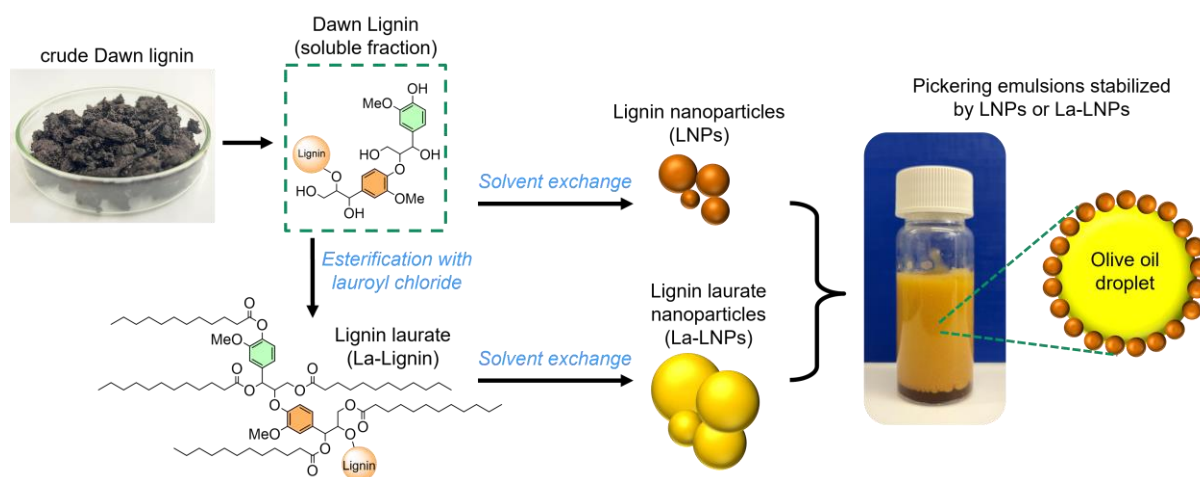
Figure 1. Schematic illustration of the present study.

2 Literature review

2.1 The challenge of lignin valorization

Lignin is one of the main components of plant biomass, alongside cellulose and hem-icellulose. This polymer is abundantly available in the biosphere, surpassing 300 bil-lion tons, with an annual increase of approximately 20 billion tons (Fernández-Rodríguez et al., 2017). The pulp and paper industry and ethanol biorefineries produce technical lignin, the form of lignin when isolated from industrial processes, amounting to 1.65 million tons per year (Dessbesell et al., 2020). However, less than 2% of this commercial production is upgraded to high-value products while the majority is burned for low-value fuel (Bajwa et al., 2019). This inefficient valorization of lignin is primarily rooted in its highly heterogeneous and complex structure.

The chemical structure of lignin is based on the enzyme-catalyzed radical coupling of its three monomeric precursor hydroxycinnamyl alcohols (also known as monolig-nols) namely, *p*-coumaryl, coniferyl, and sinapyl alcohol (Figure 2a) (Fengel & We-gener, 2011). In the lignin macromolecule, these monolignols form the corresponding structural units called *p*-hydroxyphenyl (H), guaiacyl (G), and syringyl (S) (Figure 2b) which are linked together by ether and carbon-carbon bonds (Figure 2c). The polymer-ization of the radical units occurs under chemical control (dependent on the reaction conditions) hence, there is no one well-defined structure of lignin (Ralph et al., 2004).
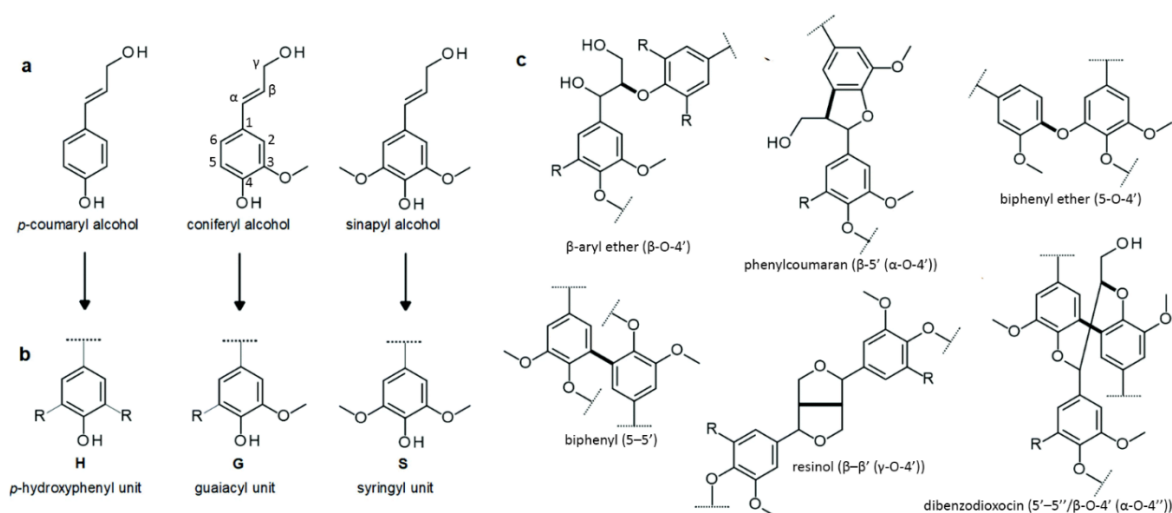
Figure 2. (a) The three monolignols and (b) their corresponding monomeric units in lignin. (c) The most common linkages in G-type lignin (adapted from Österberg et al., 2020).

The inherent heterogeneity of lignin arises from the variation in the proportion of H, G, and S units according to its botanical origin which therefore influences the relative abundance of different linkages in the macromolecule. For example, softwood lignins are predominantly composed of G units, hardwood lignins have the same proportion of G and S units with only traces of H units, and herbaceous lignins have comparable levels of G and S units but with slightly higher amounts of H units compared to hardwood lignins (Schneider et al., 2021). Regardless of origin, the β-O-4 bond is the most abundant accounting for more than 50% of the total linkages although this amount differs among plant sources (Ralph et al., 2019).

The complexity of the lignin structure is further influenced by the chemical reactions it undergoes during isolation and biomass pretreatment processes. Figure 3 illustrates the fate of native lignin during specific fractionation conditions. The resulting technical lignins can exhibit variations in bond cleavage, molecular weight, functional group compositions, and degree of condensation, depending on the specific process employed (Ekielski & Mishra, 2020).

For example, Kraft processes depolymerize native lignin via both alkaline and sulfidolytic cleavage of α- or β-O-4 linkages (Gierer, 1980). High molecular weight fragments are obtained due to parallel condensation reactions that occur mainly at C-5 positions of the aromatic rings. This reaction also results in alkali soluble fragments with covalently bonded sulfur species (Figure 3) limiting the suitability of Kraft lignin towards catalytic depolymerization (Schutyser et al., 2018). Hence, a lignin stream with minimized condensation and impurities is the goal in the design of new biorefineries (Mishra & Ekielski, 2019). Overall, the high variability among technical lignins represents a major constraint towards their transformation into high value products.

The need for lignin valorization is heightened with the advent of lignocellulosic biorefineries which are anticipated to introduce thousands of tons of technical lignins (Beckham et al., 2016). The co-production and utilization of the lignin streams are deemed to be crucial for the economic success of this sector (Bajwa et al., 2019; Xu et al., 2021).
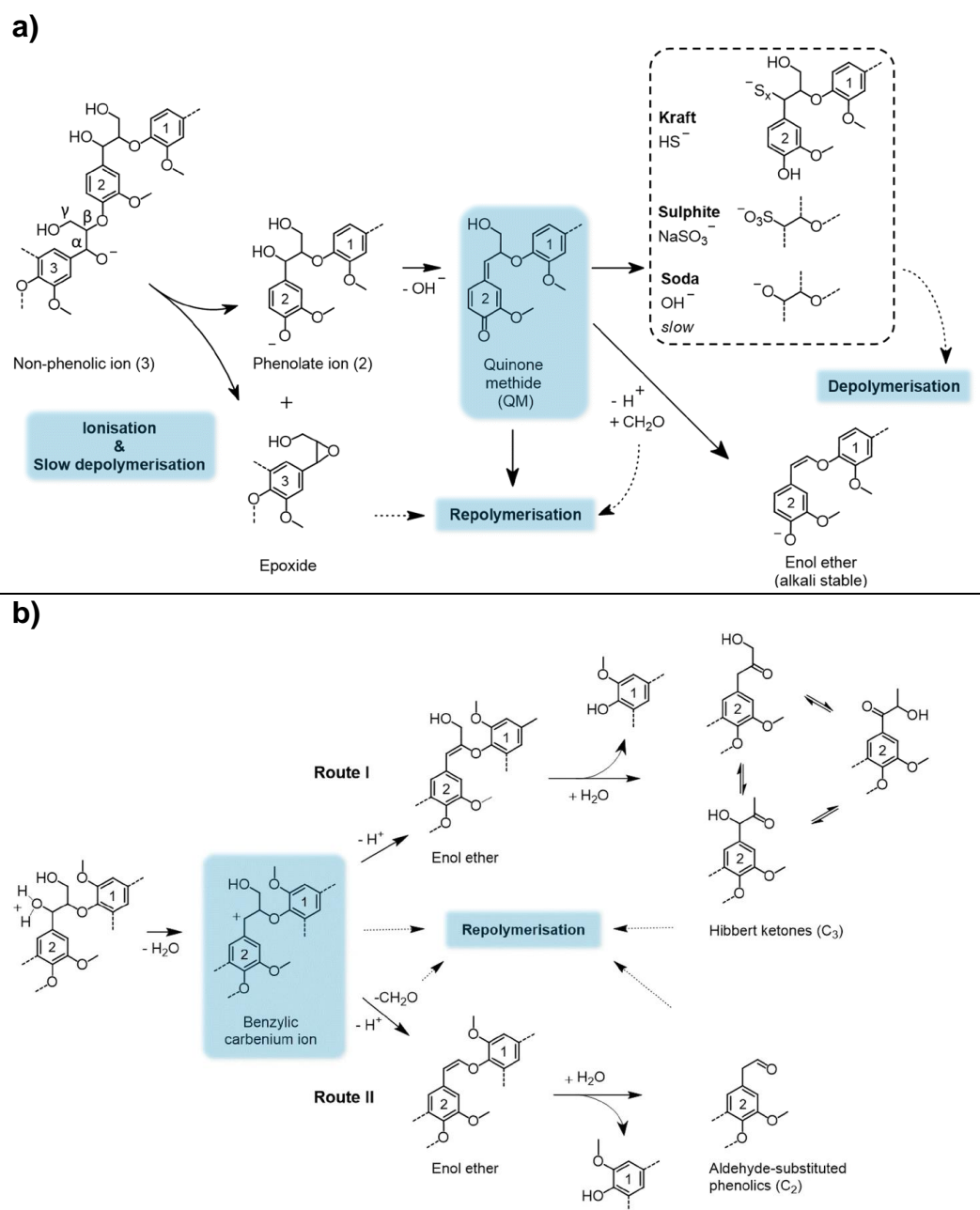
Figure 3. The cleavage of β-O-4 in native lignin during fractionation: a) base-catalyzed reactions, and b) acid-catalyzed reactions (adapted from Van den Bosch et al., 2018).

In this regard, Avantium has recently launched Dawn Technology™ pilot plant in the Netherlands which uses acid hydrolysis to convert non-food biomass into industrial sugars and lignins. During the process, the lignocellulosic material is treated with highly concentrated hydrochloric acid (40 to 51 wt%) at around 30 °C , enabling complete recovery of the biomass components as hydrolyzed sugars and solid lignin (Van Putten et al., 2019). The resulting lignin stream is highly attractive for biomedical or cosmetic applications, as it is free from sulfur, unlike the industrially dominant ligno-sulfonates and Kraft lignin. Downstream processes that can be effectively integrated

into biorefineries are currently being developed, such as utilizing soluble fractions of crude Dawn lignin as precursor materials for chemical modification and preparation of nanoparticles (Portes Abraham Silva, 2022; Wang, 2022).

2.2 Lignin esterification

Unmodified lignin has been directly used in many applications such as adsorbents (Ge & Li, 2018), precursor for carbon fibers (Kadla et al., 2002), and component in polymer blends (Doherty et al., 2011). However, for the latter, polymer blends with lignin usually exhibit inferior mechanical properties compared to the neat polymer. This is attributed to the extensive hydroxyl groups in lignin (Figure 4) which make it poorly compatible with non-polar matrices (Luo et al., 2017). Hence, chemical modification of these hydroxyl groups is a typical strategy to circumvent this issue.
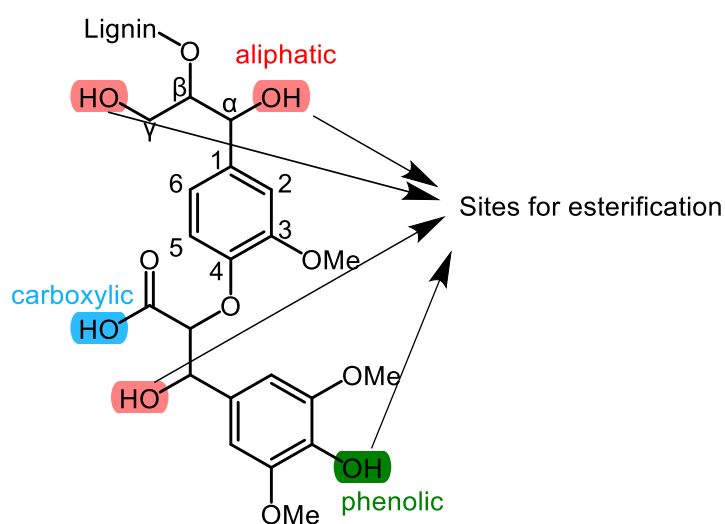
Figure 4. The different hydroxyl groups in lignin. Aliphatic and phenolic hydroxyls can be modified through esterification reactions.

Lignin is rich in hydroxyl groups, either phenolic, aliphatic, or carboxylic (Figure 4). The phenolic and aliphatic groups can be modified to create diverse derivatives of lignin (Figueiredo et al., 2018). Among the extensively studied approaches, esterification stands out due to its relatively mild reaction conditions (Laurichesse & Avérous, 2014). Ester linkages are formed through condensation reactions of the hydroxyl groups (aliphatic or phenolic) with an esterification agent such as carboxylic acid, acyl chloride, or acid anhydride. The latter two are preferred due to their higher reactivity (Duval & Lawoko, 2014). Furthermore, the selective modification of the hydroxyl

groups can also be influenced by using different catalysts: triethylamine favors phenolic hydroxyls while pyridine favors aliphatic hydroxyls (Guo et al., 1992).

Previous studies on the esterification of lignin have primarily focused on tailoring its polarity or enhancing its compatibility with non-polar polymers. For instance, acetylation of lignin has been shown to improve its solubility in THF which is useful for chromatographic analyses (Asikkala et al., 2012). Similarly, esterification of lignin with acid anhydrides of varying chain lengths has been found to increase its solubility in nonpolar solvents (Thielemans & Wool, 2005). Luo et al. (2017) esterified softwood Kraft and agricultural fiber soda lignin using C_2–C_6 anhydrides and used it to improve the tensile strength and elongation at break of thermoplastic blends. The potential of lignin palmitate and laurate as paperboard coatings has been demonstrated by Hult et al. (2013), while Nadji et al. (2009) have utilized lignin stearates as lubricants for polyethylene processing. Moreover, the modification of lignin through esterification can also lead to changes in its thermal properties, offering opportunities to enhance the melt flow characteristics of polymer blends (Koivu et al., 2016).

2.3 Lignin nanoparticles

The transformation of technical lignins into lignin nanoparticles (LNPs) have gained significant attention in recent years as this overcomes the challenge of the complex and heterogeneous chemical structure of lignin (Österberg et al., 2020; Schneider et al., 2021). Lignin nanoparticles have several advantages compared to their bulk counterpart such as their large surface area per mass unit, tunable surface properties, well-defined morphology, and improved dispersibility in aqueous media. These properties enhance their desirability for a range of applications, including bulk uses such as adhesives and dispersants, while also expanding their potential in areas such as drug delivery and catalysis (Österberg et al., 2020).

Among the numerous methods reported for the fabrication of LNPs, solvent exchange is the most dominant one due to its simplicity, scalability, and excellent control over the particle features (Lievonen et al., 2016; Österberg et al., 2023). Hence, only this method will be discussed in more detail here. Solvent exchange, also termed as solvent shifting or nanoprecipitation, is based on the intrinsic tendency of lignin molecules to self-assemble into spherical particles to reduce the surface area in contact with an antisolvent (Österberg et al., 2020). This method involves the dissolution of

lignin in an appropriate low-polar organic solvent followed by the introduction of a large amount of anti-solvent, usually water. As depicted in Figure 5, the more hydrophobic lignin molecules start the aggregation process forming the core of the particle while the more hydrophilic fractions arrange on the surface (Qian et al., 2014; Tian et al., 2017). The carboxyl groups create a negative surface charge imparting colloidal stability to LNPs via electrical double layer repulsion (Lievonen et al., 2016). Rotary evaporation or dialysis is typically employed to complete the colloidal formation, and the former is favorable for the recovery and recycling of the organic solvent (Leskinen, 2017a; Qian et al., 2014; Sipponen et al., 2018).
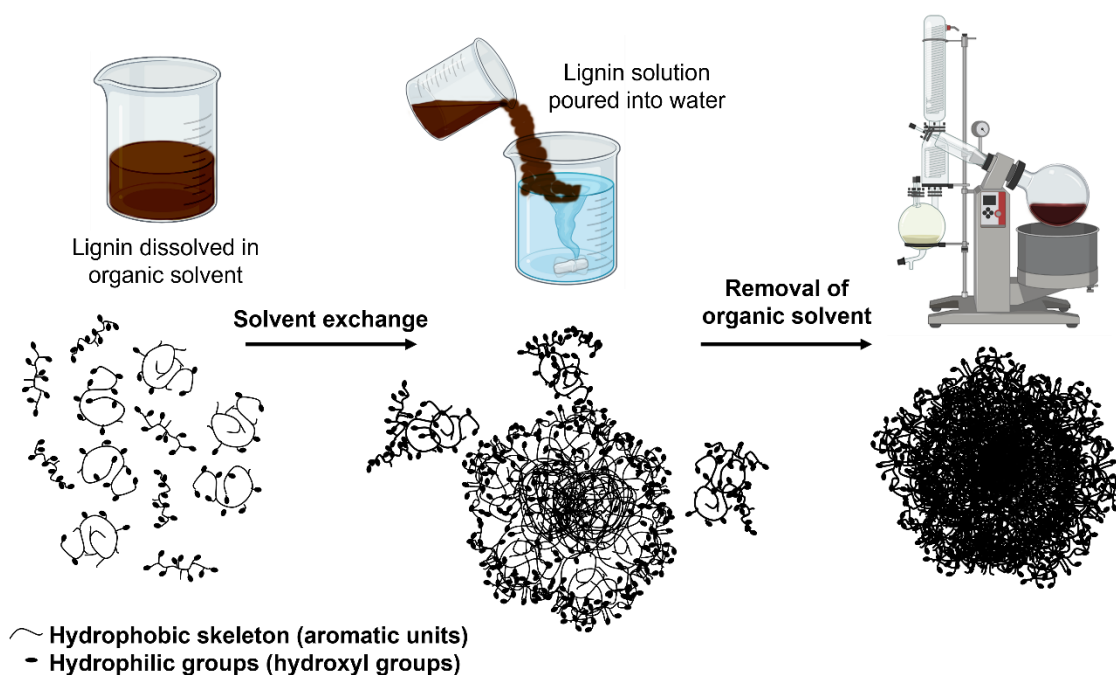
Figure 5. Schematic illustration of the self-assembly of amphiphilic lignin into spherical particles during the solvent exchange method.

Research is underway to better understand the mechanism of LNP formation and the several factors that affect the properties of LNPs, particularly in solvent exchange (Figure 6). Notably, noncovalent interactions play a vital role in the aggregation of lignin (Österberg et al., 2023). These forces include π–π stacking, van der Waals, hydrogen bonding, and hydrophobic interactions. For instance, it has been recently shown that for lignins with similar molecular weights, the difference in the sizes of their corresponding LNPs was attributed to their chemical structure. The type of intra-molecular π–π stacking differed with respect to the lignin structure (Pylypchuk et al., 2023). Additionally, it is generally understood that lignins with higher molecular weights would produce smaller particles due to the increased hydrophobic interactions and

low solubility in water (Österberg et al., 2020). Therefore, the diverse structural motifs, chemical composition, and molecular weights of different technical lignins would impact their self-assembly into nanoparticles. More knowledge on these interactions and the numerous factors that influence them would help optimize the production of LNPs.
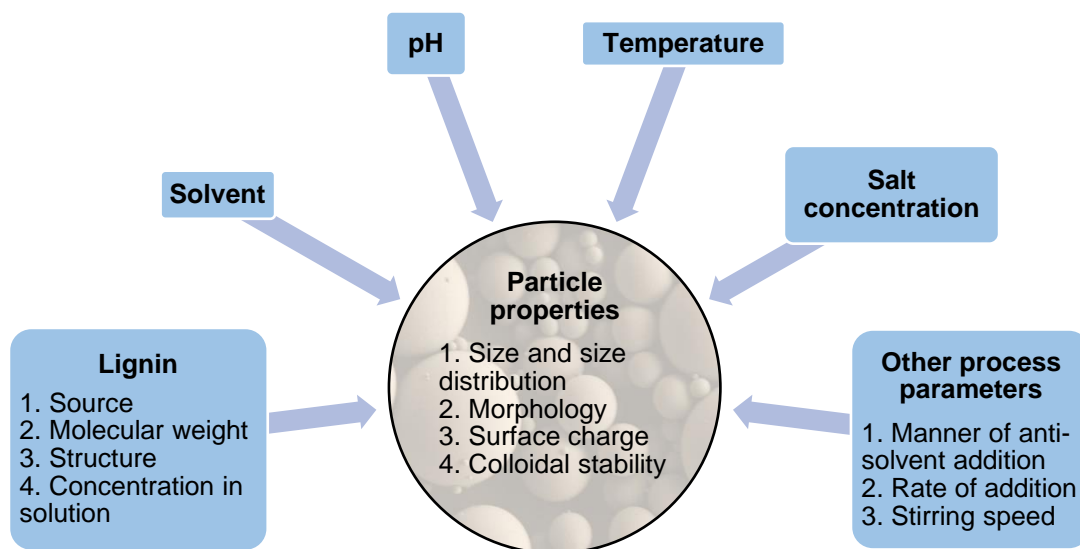
Figure 6. Factors that affect the properties of LNPs in solvent exchange method.

Like its bulk counterpart, LNPs can also be modified. There are two approaches to do this: 1) modifying the precursor lignin prior to LNP formation, and 2) modifying the surface of LNPs. Irrespective of the approach, the modified LNPs would have new properties that could be useful for specific applications.

Qian et al. (2014) demonstrated that the acetylation of alkali lignin could produce spheres of less than 200 nm in diameter with excellent colloidal stability. The enhanced hydrophobicity overcame the strong aggregation of alkali lignin in water, and they suggested π–π as the main driver for colloidal formation. Marchand et al. (2020) also prepared LNPs from acetylated lignin and showed its applicability for encapsulating bioactive compounds supported by molecular dynamics simulation. The introduction of long chain substituents to the precursor lignin has also been reported. Moreno et al. (2021) esterified Kraft lignin with oleoyl chloride which resulted in LNPs with enhanced stability for further functionalization via acid- and base-catalyzed reactions. These particles were applied as anticorrosion coatings and dye adsorbents. On the other hand, Setälä et al. (2020) used tall oil as esterification agent and produced modified LNPs with antimicrobial properties. The conversion of esterified lignin into

water-dispersible particles could also provide an alternative to reduce the use of organic solvents for application of hydrophobic coating (Hua et al., 2019).

The modification of the lignin structure prior to LNP formation introduces new interactions that could influence the self-assembly of the lignin molecule into nanoparticles. In particular, the hydrophobic character of LNP can be modified by introducing long chain substituents to the precursor lignin. Huang et al. (2019) prepared LNPs from esterified corncob lignin with varying alkyl chains. Larger particles were observed from esterified lignins compared to unmodified lignin although the sizes generally decreased with increasing length of alkyl chains. Authors also found that the lignin spheres exhibited porosities, with single holes found in acetylated samples and more porous structures were observed with increasing alkyl chain length. It was proposed that during the early stage of the assembly, esterified lignin would form two-dimensional bilayers with some imperfection sites. These would then curl up and continuously stack when the water content is increased resulting in porous spheres. Similarly, Li et al. (2020) also tailored the hydrophobicity of corncob lignin by alkylating the phenolic hydroxyls. The general trend observed was that by increasing the length of the alkyl chain, smaller particles are obtained. However, no comparison against LNPs from unmodified lignin was made. Neither study discussed the effect of the degree of substitution on the lignin derivatives and their resulting particles.

Contrasting findings were reported by Moreno et al. (2021) wherein LNPs from lignin oleate had bigger particle sizes compared to the ones from unmodified lignin. Authors explained that the increased particle size is due to the arrangement of the long chains into the core of the particle and added that the degree of substitution does not significantly affect the particle size. Further understanding of the colloidal formation of lignin and its derivatives would benefit from more research using different lignin sources and modification parameters.

For the second approach, modification is typically achieved by taking advantage of the anionic surface of LNPs through the adsorption of cationic materials such as chitosan (Zou et al., 2019), cationic lignin (Sipponen et al., 2017), and proteins (Leskinen et al., 2017b). The LNPs coated with chitosan or cationic lignin have demonstrated improved performance for stabilizing oil droplets in water. On the other hand, the adsorption of proteins on LNPs shows promising applicability in the biomedical and food sector. Typically, the modified LNPs exhibit larger particle sizes compared to their unmodified counterpart since the surface was tailored after the particles were formed.

2.4 Pickering emulsions based on lignin nanoparticles

Emulsions are colloidal dispersions of two immiscible liquids like oil and water stabilized by an emulsifying agent. These systems are essential in many applications, including food, pharmaceuticals, and cosmetics. However, conventional surfactants used to stabilize emulsions are often derived from non-renewable resources and are environmentally persistent (Badmus et al., 2021). Lignin nanoparticles can provide an interesting alternative to these traditional surfactants by the formation of Pickering emulsions. The use of LNPs as emulsifiers offers the advantages of being biobased, non-toxic, and potentially biodegradable (Österberg et al., 2020).

Pickering emulsions are a specific type of emulsion in which solid particles stabilize the interface between oil and water and this mechanism renders the system more stable against coalescence compared to its surfactant-stabilized counterpart (Li et al., 2022). The adsorption of the particles at the interface is influenced by their partial wettability in both oil and water phases, which is measured by the water contact angle (θ). As depicted in Figure 7, particles with higher hydrophilicity ($\theta < 90°$) tend to form oil-in-water (O/W) emulsions, while particles with higher hydrophobicity ($\theta > 90°$) form water-in-oil (W/O) emulsions (Kralchevsky et al., 2005). The amphiphilic nature of LNPs makes them suitable Pickering stabilizers for different emulsion systems.
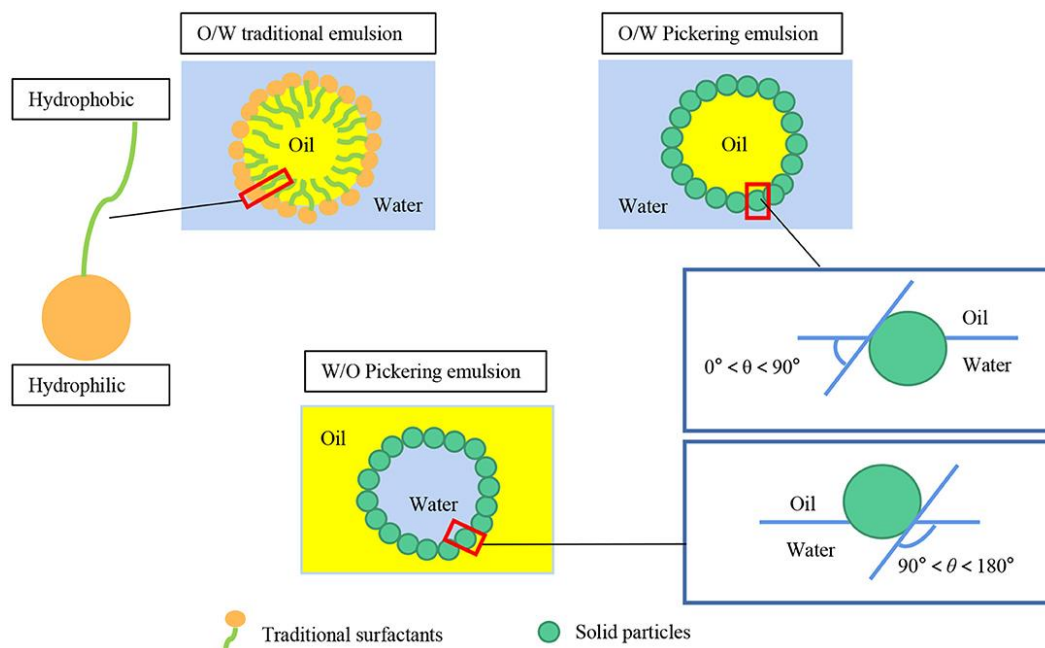
Figure 7. Comparison between traditional emulsion and Pickering emulsions. The partial wettability of the solid particle in Pickering emulsions is measured by the water contact angle (θ) (Li et al., 2022).

Table 1 shows studies on different Pickering emulsion systems using various LNPs, oils, and experimental parameters. The list focuses on emulsions stabilized by lignin particles which are nano-sized and have spherical morphology. A wide range of oils have been stabilized by LNPs. Ago et al. (2016) demonstrated the use of spherical lignin particles produced from aerosol flow reactor to stabilize emulsions of kerosene. Authors noted that the stability of the emulsions is dependent on the particle size, concentration, and water contact angle. Smaller particles and high particle concentration tend to form more stable emulsions due to the high number of adsorbed particles at the O/W interface, whereas less hydrophilic particles form emulsions that are prone to droplet coalescence.

Table 1. Pickering emulsions stabilized by lignin-based nanoparticles.

Lignin particle	Particle size	LNP loading	Type of oil	Emulsion type	Reference
Lignin particles produced from aerosol flow reactor	30 nm to 2 μm	0.1 to 0.6 wt%	kerosene	O/W	(Ago et al., 2016)
LNPs from OS, AL, and EH lignin	80–320 nm (DLS); 27-54 nm (SEM)	4.85 wt%	shea butter-babassu oil mixture, medium chain triglycerides	O/W	(Tomasich et al., 2023)
LNPs from SKL	183.6 nm	0.70 to 3.50 wt%	orange, coconut, paraffin	O/W	(Gordobil et al., 2023)
Cationic LNPs from SKL	274 nm	0.25 to 0.75 wt%	toluene, olive oil, silicone oil	O/W	(Sipponen et al., 2017a)
Chitosan-coated LNPs from SKL	113 nm	0.2 to 1.0 wt%	Olive oil	O/W	(Zou et al., 2019)
Cationic LNPs from SKL	129 nm	0.2 to 2 wt%	polycaprolactone in toluene	O/W	(Kimiaei et al., 2022)

LNPs = lignin nanoparticles, SKL = softwood Kraft lignin, OS = organosolv, AL = alkali, EH = enzymatic hydrolysis

The LNPs produced from various technical lignins were also found to stabilize shea butter-babassu oil and medium chain triglycerides (Tomasich et al., 2023). Gordobil et al. (2023) used LNPs to prepare Pickering emulsion with orange, coconut, and paraffin oil for sunscreen applications. Higher LNP concentration and oil-to-water volume fraction led to the stability of emulsions which were monitored for over 120 days.

Interestingly, the improved SPF value of the emulsion was attributed to synergistic effects between LNPs and vegetable oils. These findings exhibit the potential of LNP-stabilized emulsions in the cosmetics sector.

Surface modification of LNPs have also been shown to enhance their emulsification performance. Sipponen et al. (2017) reversed the surface charge of LNPs by adsorbing cationic lignin onto its surface. More stable emulsions were observed compared to those stabilized by unmodified LNPs. In an effort to use more biocompatible materials which are of utmost relevance in drug delivery systems, Zou et al. (2019) used chitosan to coat LNPs (chi-LNPs). These chi-LNPs were proven to effectively emulsify triglycerides which are suitable solvents for lipophilic drugs (Kalepu et al., 2013).

Lastly, the ability of LNPs to reduce interfacial tension between different phases has also been demonstrated in material design. Kimiaei et al. (2022) utilized Pickering emulsion strategy to prepare a nanocomposite of cellulose nanofibrils (CNF) and a hydrophobic polymer with LNP acting as an interfacial compatibilizer. The favorable CNF-LNP and LNP-polymer interactions resulted in the superior mechanical properties of the nanocomposite.

2.5 Contributions relative to the state of the art

Combining extensive characterization of lignin sources with the evaluation of modifications on their structure and properties would greatly benefit the development of technologies for upgrading lignin streams from biorefineries. This thesis aims to address this need by employing a range of characterization techniques, including FTIR, HSQC NMR, ^{31}P NMR, GPC, and DSC, to gain a comprehensive understanding of the new class of technical lignin introduced through the Dawn Technology™ process and to evaluate the effects of esterification on its macromolecular properties. Furthermore, this research seeks to shed light on the influence of the degree of substitution on particle formation, an aspect that has often been overlooked in previous studies but holds significance for gaining insights on the assembly process of esterified lignins. Moreover, this study extends its focus to explore the potential application of LNPs derived from Dawn lignin and its esters as emulsifiers for olive oil-in-water Pickering emulsions, building upon the groundwork laid by Portes Abraham Silva (2022).

3 Research material and methods

3.1 Raw materials and chemicals

Crude aspen lignin chips were obtained from Dawn Technology™ downstream processing (Avantium, Netherlands). Sodium bicarbonate (NaHCO3) used for neutralizing the crude lignin was obtained from VWR. The fractionation solvents used were tetrahydrofuran (99.9%, VWR) and ethanol (94.0%, ALTIA Oyj). The solvents and reagents used for esterification were tetrahydrofuran (99.9%, VWR), *N,N*-dimethylformamide (≥99.8%, VWR), pyridine (≥99.0%, Sigma-Aldrich), and lauroyl chloride (≥97.5%, Sigma-Aldrich). Celite 535 used for the reaction workup was obtained from Sigma-Aldrich. Deionized water was used throughout the experiments. Olive oil (Borges Extra Virgin Oliiviöljy) was used for Pickering emulsion studies.

3.2 Lignin Fractionation

The crude lignin chips received were highly acidic (pH = 1.5), so these were neutralized first. Six hundred grams of crude lignin was washed with 1000 mL of deionized water thrice and vacuum-filtered after every washing. Afterwards, the chips were dispersed in 1000 mL of deionized water and a saturated solution of 100 mL NaHCO3 was added to the dispersion bringing the pH to 7.0. Neutralization with NaHCO3 was done once more resulting to a pH of 7.6. The chips were finally washed with 1000 mL of deionized water thrice to remove the resulting salts of the neutralization reaction. The neutralized crude lignin had a dry matter content of 12.9 %.

A tertiary solvent system of tetrahydrofuran (THF), ethanol (EtOH), and water (H_2O) was used to obtain the soluble fraction from the neutralized crude lignin. Typically, 47 g of neutralized crude lignin was weighed in a 500 mL Duran bottle and 200 mL of THF:EtOH:H_2O (4:3:3 v/v/v) was added. The dry matter content of the crude lignin was used in calculating the proportion of the solvents. The mixture was placed in an ultrasound water bath (Sonorex Digitec DT 52, Bandelin) and the sonication was performed for 30 min at 65 °C. After sonication, the mixture was filtered with a qualitative filter paper (12-15 um particle retention). The fractionation yield was obtained by evaporating the organic solvents from 10 mL of the filtrate using a rotary evaporator followed by oven-drying for 24 h. A yield of 19.0 ± 4.3 % was obtained as an average

of five fractionation batches. For simplicity, the lignin fraction soluble in this solvent mixture is referred to as Dawn lignin in this report.

3.3 Lignin Modification: Esterification

After removing the solvents by rotary evaporation, Dawn lignin was freeze-dried for 24 h to yield dry lignin powder. Lignin esterification was performed following the method described by (Koivu et al., 2016) with minor modifications (Figure 8). Briefly, 1.0 g of dry lignin (containing 5.60 mmol/g of total phenolic and aliphatic OH measured by quantitative ^{31}P NMR analysis) was dissolved in 10 mL of THF, 2.5 mL of DMF, and 0.76 mL of pyridine (9.4 mmol/1 g lignin) at 60 °C for 30 min. Afterwards, 1.73 mL of lauroyl chloride (130 mol% equiv vs total aliphatic and phenolic OH) was injected with a syringe. The reaction vessel was purged with nitrogen gas and the reaction was kept for 48 h at 65 °C with efficient stirring. Separate batches were also prepared for 70 and 30 mol% equiv vs total aliphatic and phenolic hydroxyls. In this report, the lignin laurates are referred to as La-Lignin$_{30}$, La-Lignin$_{70}$ and La-Lignin$_{130}$.
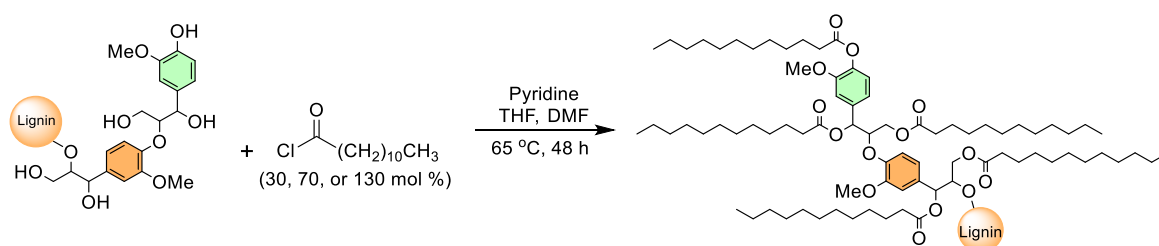
Figure 8. Scheme of the esterification of Dawn lignin with lauroyl (C$_{12}$) chloride at varying molar ratios. The lignin laurate (La-Lignin) is depicted with complete esterification at all possible aliphatic and phenolic hydroxyl groups which could be expected for the reaction with 130 mol% of lauroyl chloride.

The reaction workup was performed starting with the addition of sufficient amount of Celite 535 into the mixture to make it powdery. The mixture was then washed once with 100 mL of deionized water, and twice with 50 mL ethanol/water solution (1:1 volume ratio; cooled to 0 °C) to precipitate the product and to wash off the reaction solvents and the salts. Lignin laurate (La-lignin) was extracted using 50 mL of chloroform. The organic solvent was evaporated in a rotary evaporator to obtain the product. The La-Lignin$_{130}$ yielded a thick, oily material, while the La-Lignin$_{70}$ and La-Lignin$_{30}$ formed solid flakes (Appendix A).

3.4 Characterization of lignin and lignin laurate

3.4.1 ATR-FTIR

The major functional groups present in Dawn lignin and the La-Lignins were identified using attenuated total reflection – Fourier transform infrared spectroscopy (ATR-FTIR) (PerkinElmer, Spectrum Two FT-IR Spectrometer). Dry samples were placed on a diamond crystal plate and the spectra were recorded from 600 to 4000 cm^{-1} with a resolution of 1 cm^{-1}. The average of 10 scans per sample was used for reporting.

3.4.2 HSQC and 31P NMR

Nuclear magnetic resonance (NMR) spectroscopy was conducted using Bruker NMR Spectrometer AV III 400 MHz spectrometer. The bonding patterns of Dawn lignin and its esters were analyzed using liquid state $^{1}H-^{13}C$ heteronuclear single quantum coherence nuclear magnetic resonance (HSQC NMR). Dawn lignin and La-Lignin$_{30}$ were dissolved in deuterated dimethylsulfoxide (DMSO-d6) while La-Lignin$_{130}$ and La-Lignin$_{70}$ were dissolved in deuterated chloroform (CDCl$_3$). Around 60 mg of the dry samples were weighed and dissolved in 0.70 mL of the appropriate solvent. A total of 36 scans were performed with 2 s pulse delay (hsqcetgpsip.2 pulse sequence) at 25 °C.

Semi-quantification of the lignin signals was performed following the assumption proposed by Tarasov et al. (2022) as shown in equation 1. Authors chose G$_2$ and S$_{2,6}$ peaks as reference due to the negligible reactivity of these positions.

$$G + S = G_2 + \frac{S_{2,6}}{2} = 100 \text{ Ar} \tag{1}$$

The hydroxyl groups of the Dawn lignin and La-Lignin were quantified with ^{31}P NMR. The samples were prepared according to the method described by Koivu et al. (2016). Samples were dried in a vacuum oven at 40 °C for 24 h. Around 30 mg of the dried sample was accurately weighed in a glass vial and the following reagents were added in the order: 150 µL of dimethylformamide (DMF), 100 of µL pyridine, 200 µL of the internal standard of N-hydroxy-5-norbornene-2,3-dicarboxylic acid imine (NHND)(10.2 µmol), 50 µL of the chromium (III) acetylacetonate as relaxation agent (1.63 µL), and 300 µL of chloroform-d6. The solution was stirred with a magnetic stirrer for around 10 min. Afterwards, 150 µL of the phosphorylating agent, 2-chloro-4,4,5,5-tetramethyl-1,3,2-dioxaphospholane (TMDP) (Sigma-Aldrich), was added

dropwise. The solution was then transferred into a 5-mm NMR tube. Samples were analyzed within 30 min of phosphorylation. A total of 128 scans were performed with 1 s acquisition time and 5 s pulse delay (zgig with 90° pulse angle) at 25 °C.

The hydroxyl groups were determined by integrating the peak of the internal standard and the aliphatic, phenolic, and carboxylic hydroxyl regions as per the protocol described by Meng et al. (2019). All spectra were calibrated by shifting the signal of the TMDP and water at 132.2 ppm. The integration values were converted to mmol OH/g lignin (or La-Lignin) using equation 2, where E represents the integration ratio of the hydroxyl region to the internal standard (IS).

$$\text{mmol OH / g lignin} = \frac{E \times IS \text{ (in mmol)}}{\text{Dry weight of lignin (g)}} \quad (2)$$

In addition, the degree of substitution (DS) was calculated according to equation 3, where OH_i is the initial concentration of hydroxyl groups in lignin, and OH_f is the final concentration of the hydroxyl groups in the esterified lignin, and Δm is the weight increase (g) per gram of lignin assuming reactions are 100% complete. Both OH_i and OH_f only consider the aliphatic and phenolic hydroxyls.

$$DS = \frac{OH_i - OH_f}{OH_i + OH_f \times \Delta m} \quad (3)$$

3.4.3 GPC

The molecular weight distribution of Dawn lignin and La-Lignins was analyzed using gel permeation chromatography (GPC) (Agilent, USA). Sample preparation was done following the method described by Sipponen et al. (2017). In order to render Dawn lignin completely soluble in THF for analysis, it was acetylated using pyridine:acetic anhydride (1:1 v/v). Prior to injection, the samples were prepared at a concentration of 2 mg/mL and filtered through a 0.22 μm PTFE syringe filter (VWR). The eluent used was THF with a flow rate of 1 mL/min. A volume of 50 μL was injected into the chromatography system, which was equipped with a Phenogel pre-column (50 mm length, 7.8 mm inner diameter, and 5 μm particle size), as well as 50 Å and 1000 Å Phenogel columns (300 x 7.8 mm, 5 μm). An ultraviolet detector (280 nm) was used for monitoring. The system was calibrated using polystyrene standards with molecular weights between 953 to 68000 g/mol and toluene (92 g/mol).

3.4.4 DSC

Glass transition temperatures (T$_g$) of Dawn lignin and La-Lignins were determined using differential scanning calorimetry (DSC) (DSC 250 Auto model, TA Instruments, USA). The samples (5–10 mg) were weighed in aluminum pans and a hole was poked onto the lid to let residual solvents be released during the heating. The temperature program used a ramp speed of 10 °C/min: equilibrate to 25 °C, (first heating cycle) ramp to 200 °C, isothermal 1 min, ramp to -50 °C, isothermal one min, (second heating cycle) ramp to 200 °C, isothermal 1 min.

3.5 Preparation of lignin nanoparticles

Colloidal nanoparticles from Dawn lignin and La-Lignins were prepared via solvent exchange method. For the production of unmodified lignin nanoparticles, 200 mL of the Dawn lignin (0.5 wt%) dissolved in the THF:EtOH:H$_2$O system obtained directly from the fractionation was poured into four times higher amount of the anti-solvent, which was 400 mL of deionized water, and stirred at 500 rpm for 15 min. Afterwards, the organic solvents were removed via rotary evaporation and the dispersion was concentrated to 2 wt% at 45 °C, 25 mbar.

Lignin laurate nanoparticles (La-LNP) were also prepared in the same manner with some modifications. A concentration of 0.5 wt% of La-Lignin in THF (25 mL) was poured into five times higher amount of deionized water (125 mL) with slow stirring (~200 rpm) for 5 min. Next, the organic solvents were removed via dialysis. The dispersions were introduced into a dialysis bag (Spectra/Por® 1 Standard RC Dry Dialysis Tubing, 6–8 kDa, Spectrum Labs, USA) which was dialyzed against an excess of deionized water for 24 h. The La-LNP dispersion was centrifuged at 10000 rpm at 4 °C for 30 mins. The residue which contained the nanoparticles was redispersed in water to prepare 0.5 wt% of La-LNPs.

3.6 Characterization of LNP and La-LNP

3.6.1 Hydrodynamic Diameter and ζ-Potential Analysis

The hydrodynamic diameter (D$_h$) and ζ-potential of the LNPs and La-LNPs were measured using Zetasizer Nano ZS90 instrument (Malvern Instruments Ltd., U.K.). The nanoparticle dispersions were diluted 10x with deionized water and the pH values

were obtained before measurements. Dynamic light scattering (DLS) experiments were performed to determine the size and size distribution of the nanoparticles, and the measured Z-average (intensity-weighted mean hydrodynamic size) was reported. On the other hand, the electrophoretic mobility was measured using a dip cell probe, and Smoluchowski equation was used to calculate the ζ-potential values. Three measurements were recorded for D_h and ζ-potential, and the mean values were reported.

3.6.2 SEM

Thin films of LNP and La-LNP were prepared for morphology analysis following the method described by Farooq et al. (2020). Briefly, silica wafers were cut into 1 x 1 cm square chips to be used as substrates. These were immersed in 1 M of NaOH for 15 s, rinsed with deionized water, and then dried with compressed nitrogen gas. Afterwards, these were cleaned by UV/ozone treatment for 15 min, followed by subsequent rinsing and drying. Then, an anchoring layer of poly-L-lysine (PLL) (0.1 % w/v in H_2O, Sigma-Aldrich) was added by depositing a drop of the solution onto the wafer. The surface of the wafer was covered by the droplet for 30 min. After rinsing and drying, the LNP or La-LNP were adsorbed on top of the PLL layer for 1 h. Final rinsing with water and drying with nitrogen gas was done to remove excess material.

The nanoparticles were observed using scanning electron microscopy (SEM) (Zeiss Sigma VP, Germany) under vacuum at an accelerating voltage of 2 kV. Prior to SEM analysis, the silica wafer chips with adsorbed LNP or La-LNP were mounted on metal stubs with double-sided carbon tape. The thin films were coated with a 10-nm layer of gold-palladium alloy using a Leica EM ACE600 sputter coater.

3.7 Preparation of Pickering Emulsions

Pickering emulsions were prepared using IKA T-18 Basic Ultra Turrax homogenizer. In a glass vial, olive oil as the oil phase was mixed with the aqueous dispersion of LNP or La-LNP in o/w volume ratio of 1:1. The mixture was homogenized at 12 000 rpm for 2 mins. Characterizations of the emulsions were conducted 3 h after preparation, following the limited coalescence phenomena (Arditty et al., 2003).

Due to the observed ability of the LNP to stabilize olive oil in water, a more detailed study was done to evaluate the effect of LNP loading on the stability of the emulsions.

Same procedures for preparing emulsions were followed but the concentration of LNP was varied to 0.25, 0.5, 1.0, 1.5, and 2.0 wt%.

Images of the emulsion oil droplets were captured using an optical microscope (Olympus BX53M). For olive oil-in-water emulsions stabilized by LNP, the mean droplet diameter was measured based on volume data volume data (d43, De Brouckere Mean Diameter) using laser diffraction (Malvern Mastersizer 2000, U.K.). The mean value of 30 measurements were used for the reporting of data.

4 Results and discussion

4.1 Esterification of Dawn lignin with lauroyl chloride (C_{12})

The successful esterification of Dawn lignin was monitored by FTIR-ATR as illustrated in Figure 9. The OH band at 3380 cm^{-1} progressively decreased indicating the reaction of the hydroxyl groups in the lignin macromolecule. Furthermore, the intensification of C=O stretching bands confirms the formation of ester linkages in lignin: the sharp increase at 1705 cm^{-1} arises from the esterified aliphatic hydroxyls and the emergence of another band at 1738 cm^{-1} is attributed to the esterified phenolic hydroxyls (Zhao et al., 2017). The relative intensity of the C=O bands also increased with increasing molar ratio of lauroyl chloride. Lastly, the C-H stretching at 2846 and 2915 cm^{-1} also intensified which indicates the incorporation of the long alkyl chain of lauric acid.
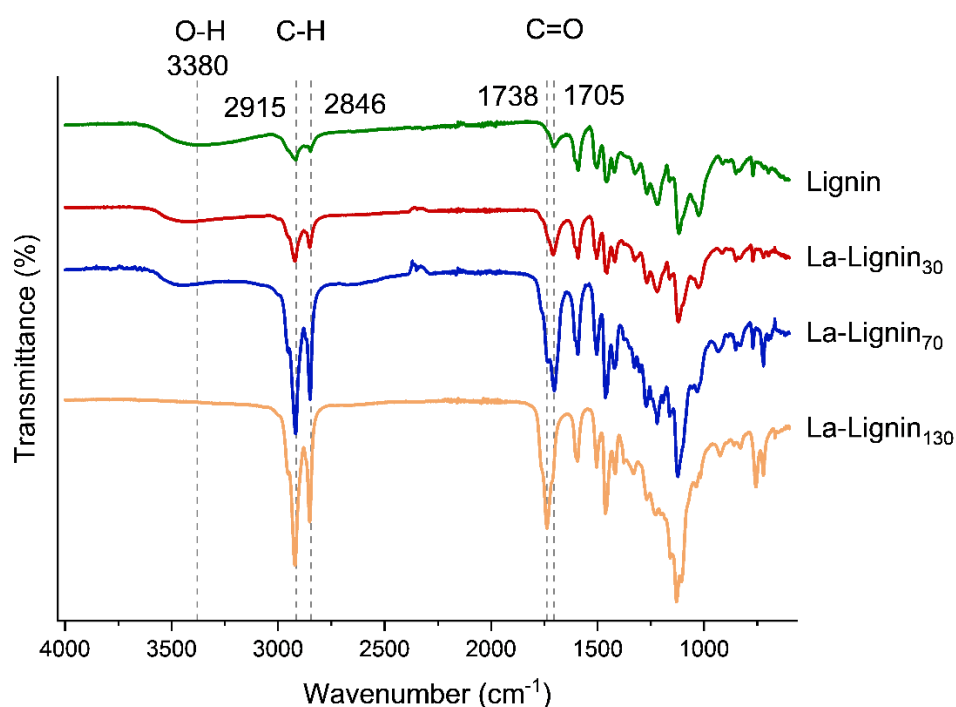
Figure 9. Stacked FTIR transmittance spectra of Dawn lignin and the La-Lignins with signal assignments.

The structural features in the Dawn lignin fraction were identified using HSQC-NMR as shown in Figure 10a. The signals at δ_H/δ_C 6.0–8.0/100–140 ppm correspond to the aromatic units present in Dawn lignin (Figure 10a). As expected for hardwood lignins, syringyl (S) and guaiacyl (G) units were abundant, with small amounts of p-hydroxybenzoate groups as side chain γ-esters typical in aspen lignins (Ralph &

33

Landucci, 2010). Semi-quantification by HSQC NMR approximated a S/G ratio of 1.6 which agrees to the range of values reported for hardwood lignins (1.01 to 1.68) (Bose et al., 2009). In addition, the amounts of p-hydroxybenzoate units were about 23 per 100 Ar.
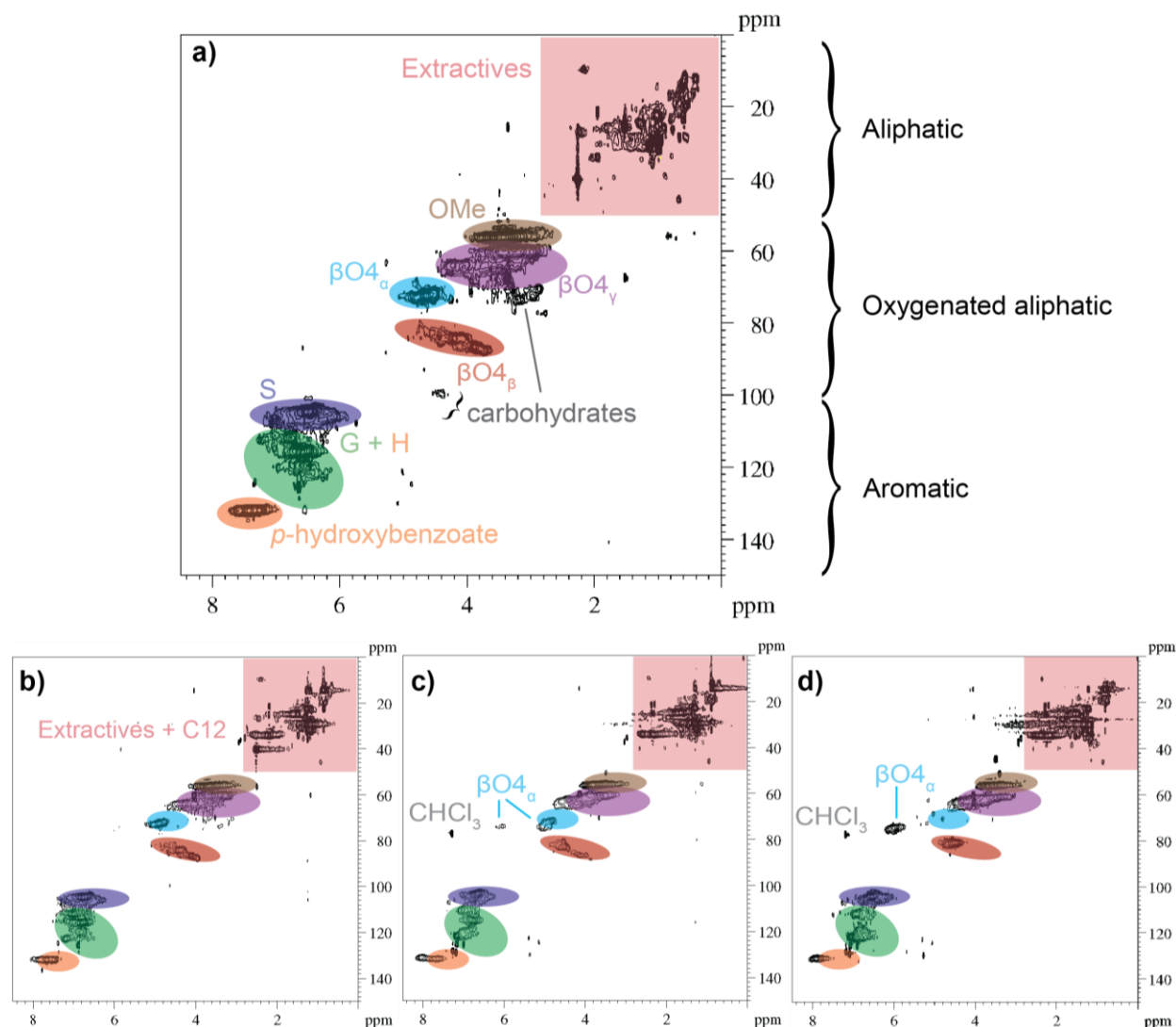
Figure 10. HSQC-NMR spectra of Dawn lignin and La-Lignins with corresponding signal labels. a) Dawn lignin, b) La-Lignin$_{30}$, c) La-Lignin$_{70}$, and d) La-Lignin$_{130}$. Colored markings in the Dawn lignin spectra are retained at the same positions in b–d to highlight changes in signals.

The oxygenated aliphatic region was shown at δ_H/δ_C 2.5–6.0/50–100 ppm. Relatively high amounts of β-O-4 signals were detected, and it was estimated that this linkage was present at about 46 per 100 Ar. The number of β-O-4 linkages in hardwood lignins is typically around 50–65 per 100 Ar (Li et al., 2015). Hence, these findings suggest that the hydrolysis process of Dawn Technology™ preserved these native aryl

ether linkages. Methoxyl signals were also visible at δ_H/δ_C 2.5–4.0/50–60 ppm due to the methoxylated S and G units present (Ralph & Landucci, 2010).

Some impurities were detected in the fraction. There were residual carbohydrates which corresponding signals at δ_H/δ_C 2.8–3.6/70–80 ppm and δ_H/δ_C 4.4/100 ppm (Hedenström et al., 2009). In addition, the aliphatic region (δ_H/δ_C 0–2.5/0–50 ppm) showed various signals which could be attributed to the fatty acid extractives that were soluble in the fractionation solvent system (Bogolitsyn et al., 2014).

Changes in the lignin structure after esterification were also identified. The progressive shift to lower field (shift to higher ppm) of the ^1H signals of aromatics, β-O-4$_\alpha$, and β-O-4$_\gamma$ signify substitution of the OH groups at these positions with fatty acid chains (Figure 10b–d). It can be inferred from Figure 10b that the significant shift of the β-O-4 γ-signals compared to β-O-4 α-signals could be attributed to the higher reactivity of the less sterically hindered primary OH at γ position (Fox et al., 2011). At 130% molar ratio, almost complete esterification of the α-OH was hinted by the total shift of the β-O-4 α-signal of La-Lignin$_{130}$. Moreover, the narrowing of β-O-4 β-signals with increasing esterification (Figure 10b–d) could be attributed to the increasing homogeneity of its electronic environment. Finally, signals in the aliphatic region also became broader which could be due to the C_{12} fatty acid side chains (Wen et al., 2017).

To further validate the esterification of Dawn lignin, the hydroxyl contents of Dawn lignin and the lignin laurates (La-lignin) were calculated via ^{31}P NMR analysis. This technique involves the phosphitylation of the OH groups with TMDP, and then quantitatively assessing their signals against an internal standard (Meng et al., 2019). Figure 11 compares the spectra of Dawn lignin and a representative lignin laurate (La-Lignin$_{70}$) with signals assigned to aliphatic, phenolic, and carboxylic OH present in the macromolecules. A detailed list of OH contents of Dawn lignin and La-Lignins is shown in Table 2. Reduction of signals from the aliphatic and phenolic OH groups were evident from the spectrum of La-Lignin which further confirms the esterification of lignin. On the other hand, the carboxylic OH contents of the La-Lignins were higher than that of the starting lignin (Table 2). This was possibly due to the unreacted lauroyl chloride which was hydrolyzed into fatty acids during the workup.
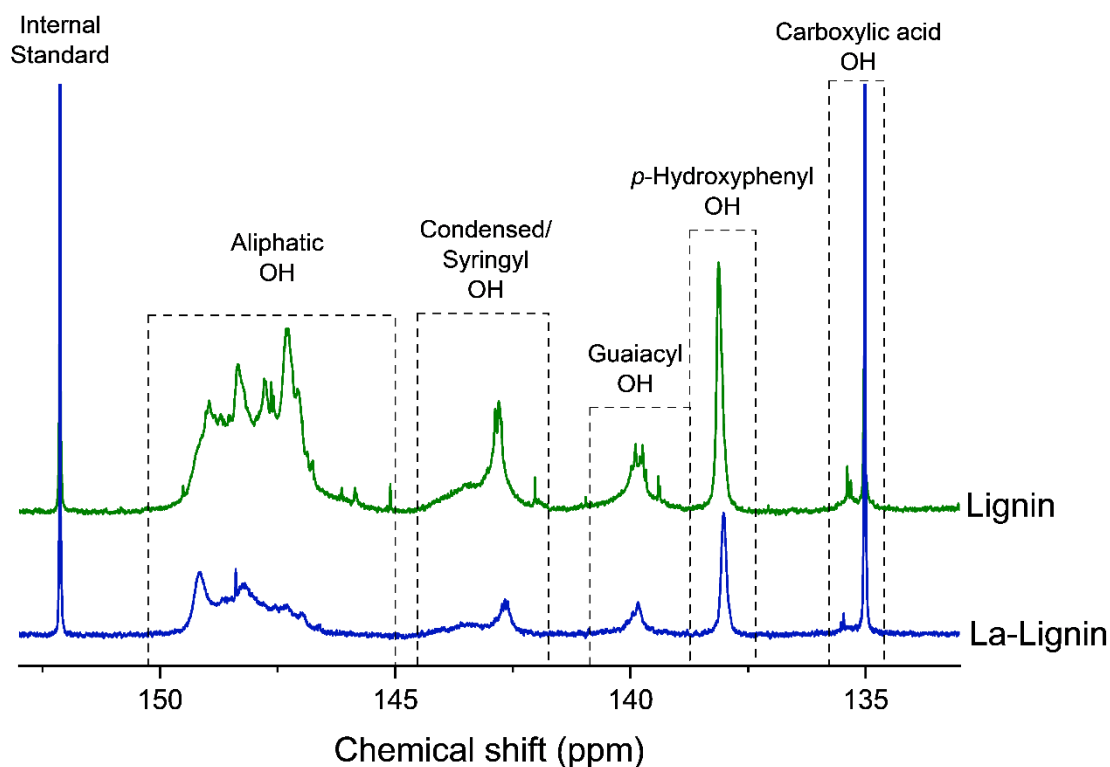
Figure 11. Quantitative ^{31}P NMR spectra of Dawn lignin and La-Lignin$_{70}$ phosphitylated with TMDP using NHND as internal standard.

Table 2. Total hydroxyl contents (in mmol/g of sample) and degrees of substitution (DS) of Dawn lignin and the La-Lignins.

OH content in mmol/g	Lignin	La-Lignin$_{30}$	La-Lignin$_{70}$	La-Lignin$_{130}$
Aliphatic OH	3.79	2.08	0.92	0.01
Phenolic OH	1.87	1.25	0.52	0.01
• Condensed/Syringyl	0.84	0.60	0.20	0.01
• Guaiacyl	0.45	0.30	0.12	0
• p-Hydroxyphenyl	0.58	0.36	0.20	0
Total$_{aliphatic + phenolic}$	5.66	3.33	1.44	0.02
Carboxylic	0.20	0.65	0.56	0.46
DS$_{Aliphatic}$ (%)	-	39	65	100
DS$_{Phenolic}$ (%)	-	20	56	100
Total DS (%)	-	35	63	100

The degree of substitution (DS) of the aliphatic and phenolic OH was estimated by comparing the OH contents in the La-Lignins against the OH groups in the starting Dawn lignin (Table 2). This approximation assumes that esterification reactions are 100% complete (Koivu et al., 2016). Quantitative esterification (100% DS) was achieved when 130 mol% of lauroyl chloride to total OH ratio was used. Meanwhile a

DS of 35 % and 63 % was obtained with 30 mol% and 70 mol% lauroyl chloride loading, respectively. Ideally, the achievable DS is limited by the molar ratio of acylating reagent added. However, a higher experimental DS value for La-Lignin$_{30}$ was calculated which could be a result of the reaction workup. The less substituted, more polar lignin esters may have remained undissolved in the nonpolar chloroform which was used for the extraction. This workup yielded extracts containing lignin esters with a higher DS as measured from ^{31}P NMR analysis.

The selective reactivity of hydroxyl groups was also compared. The DS of the aliphatic and phenolic OH in La-Lignin$_{30}$ and La-Lignin$_{70}$ shown in Table 2 suggests preferential reactivity towards aliphatic OH. This preference is probably due to primary aliphatic OH being less sterically hindered than phenolic OH. These findings agree with the results of Koivu et al. (2016) where they esterified softwood Kraft lignin (SKL) with long chain fatty acid chlorides. Furthermore, it has been shown that pyridine catalysis favors aliphatic OH in model compounds (Guo et al., 1992).

From the GPC results shown in Figure 12, the changes in molecular weight of Dawn lignin after esterification were evaluated. The chromatograms of the La-Lignins increasingly shift to higher molecular weights with increasing DS. Moreover, the polydispersity of the La-Lignins were lower than that of Dawn lignin and shows a decreasing trend with decreasing DS. It is expected that the chloroform extraction during the workup resulted to less-substituted lignin esters remaining undissolved due to their higher relative polarity.

An increase in molar mass values was monitored for La-Lignin$_{70}$ and La-Lignin$_{130}$ which is a result of the linkage of the C_{12} chains into the lignin backbone although this effect was not the same for La-Lignin$_{30}$. The chromatogram of La-Lignin$_{30}$ shows that the unextracted lignin esters are of high molecular weight fractions resulting in lower molar mass values of La-Lignin$_{30}$ in comparison to Dawn lignin.

With the same chloroform extraction work up applied to all esterification batches, increasing yield was obtained with increasing DS: La-Lignin$_{30}$ with 77% yield, La-Lignin$_{70}$ with 81% yield, and La-Lignin$_{130}$ with 90% yield. The esterification of lignin with a long chain fatty acid decreases its polarity and therefore affects its solubility in different solvents (Thielemans & Wool, 2005). In this case, increased DS resulted in higher yields with the nonpolar chloroform as the extraction solvent. Overall, substitution of OH groups with fatty acid side chains increases the molecular weight and consequently decreases the polarity of lignin esters.

37
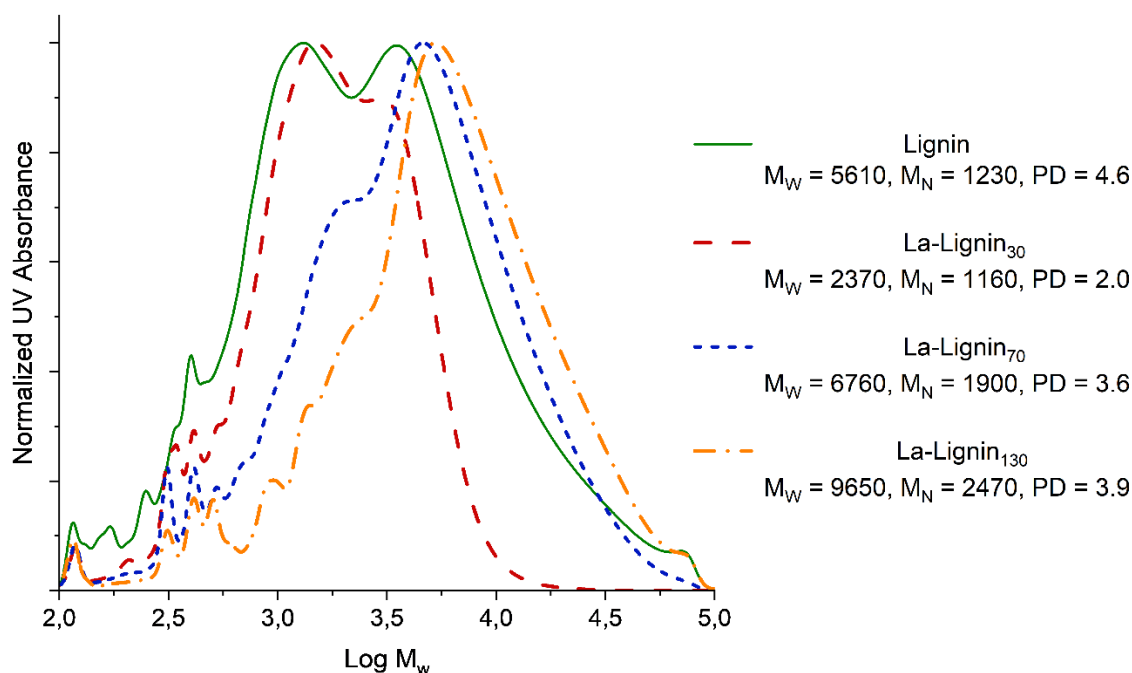
Figure 12. Molecular weight distribution of Dawn lignin (acetylated) and La-Lignins. Weight-average molar mass (M_W) and number-average molar mass (M_N) values are in g/mol while the polydispersity is M_W/M_N.

Dried La-Lignin$_{30}$ and La-Lignin$_{70}$ appeared as solid flakes or powders while La-Lignin$_{130}$ appeared to be a tacky material (Appendix A). These observations hinted that the incorporation of long chain fatty acids into the rigid lignin macromolecule could affect its thermal properties.

To investigate this further, differential scanning calorimetry (DSC) was conducted to evaluate the effect of the degree of substitution on the glass transition temperature (T_g) of Dawn lignin as depicted in Figure 13a. Dawn lignin exhibited a T_g of 100 °C which is slightly lower compared to values reported in literature for hardwood lignins (Börcsök & Pásztory, 2021). When esterified, two thermal transitions were observed: one at the original T_g for unmodified lignin and another one at a lower temperature. Clear melting endotherms were observed for La-Lignin$_{70}$ and La-Lignin$_{130}$ at 34 °C and 24 °C, respectively, while a less pronounced peak was also observed for La-Lignin$_{30}$ at 35 °C (Figure 13a). These thermal transitions were also visible for both first and second measurement cycles indicating their reversible nature (Figure 13b). This increased molecular mobility at low temperature could explain the glue-like behavior of La-Lignin$_{130}$.
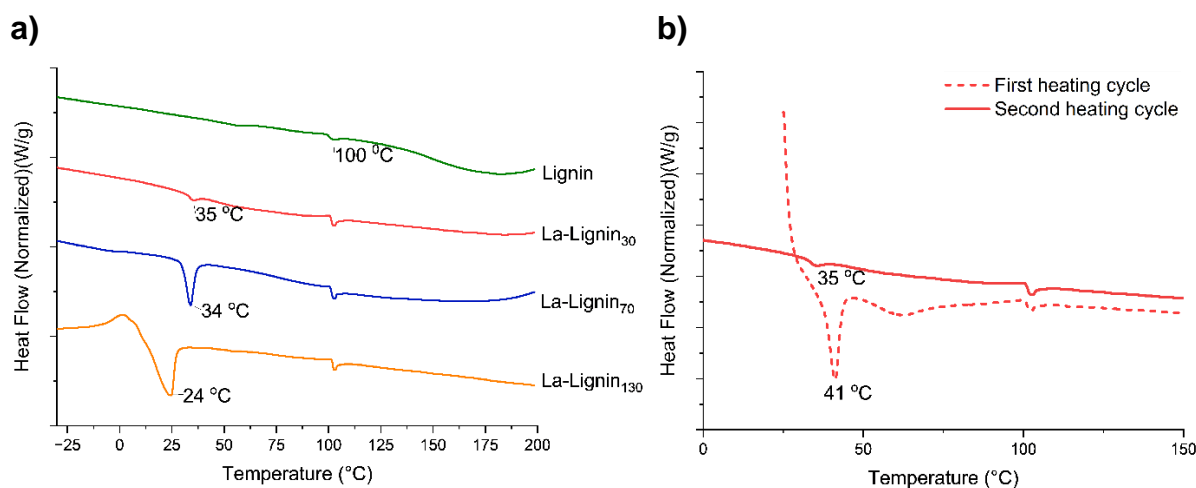
Figure 13. DSC thermogram for Dawn lignin and La-Lignins: a) second heating cycles of the four samples and b) a comparison between the first and second heating cycle of La-Lignin$_{30}$.

Previous studies have shown the crystalline behavior of lignin esterified with long chain substituents. Pawar et al. (2016) first reported this melting transition of highly esterified lignins. They made similar observations in which above 95 mol% substituted C_{18} Kraft lignin esters exhibited melting points (T_m) at 48 °C and 31°C during the first and the second heating cycle, respectively. On the other hand, Koivu et al. (2016) observed irreversible melting endotherms only for 10–50 mol % C_{16} KL esters. However, these transitions were present at higher temperatures between 120 and 130 °C. Koivu et al. also performed esterification of SKL with C_8 and C_{12} fatty acid chlorides, but they did not report melting transitions for these lignin esters. Nevertheless, both hypothesized that these phenomena are due to the crystallization of the long fatty acid chains as depicted in Figure 14.
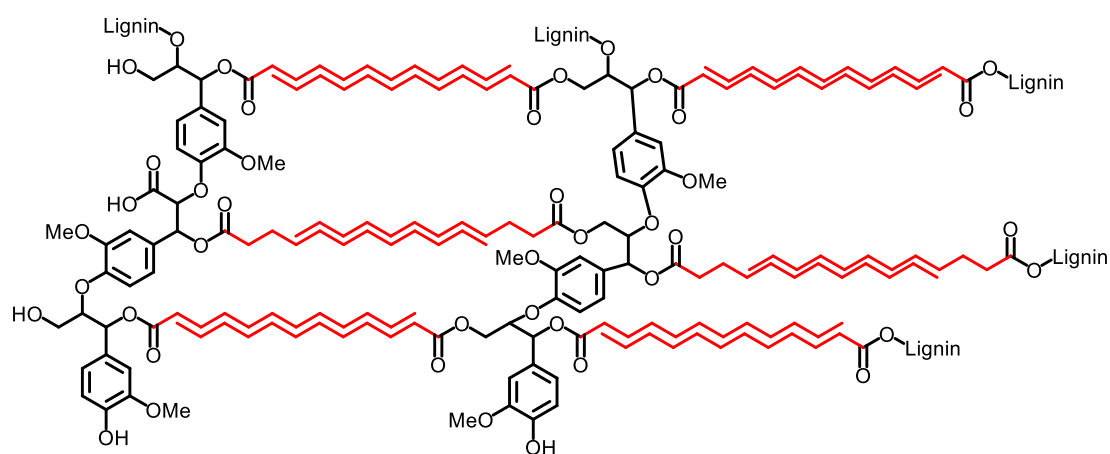
Figure 14. Illustration of the possible crystalline packing of the C_{12} side chain of lignin laurate.

The high T_g of lignin is a result of its rigid phenolic moieties and strong intermolecular hydrogen bonding (Gordobil et al., 2023). The long fatty acid chains in esterified lignin pack together in a crystalline manner by van der Waals forces thereby resulting to a melting transition (Siram et al., 2019). Despite lauric acid having a T_m of 43.2 °C, it is possible that the esterification of this substituent to lignin resulted in some restrictions in its orderly packing hence, a lower T_m was measured. The broad melting range at lower temperatures most evidently observed in La-Lignin$_{130}$ could probably be attributed to the combined effects of the heterogeneous structure of lignin and the increased free volume introduced by the C_{12} chains (Luo et al., 2017). It is also possible that the residual lauric acid could have an effect in this melting behavior.

The cause for the consistent occurrence of a thermal transition at 100 °C in all samples is still unclear. All samples underwent a first heating cycle which was supposed to remove any moisture or residual solvents. This finding could be due to the structural motifs in Dawn lignin although further investigation is needed to understand this.

A cold crystallization peak was also observed in La-Lignin$_{130}$. It was previously reported that C_2–C_6 could induce cold crystallization in PHBV blends although the reason behind remains unexplored (Luo et al., 2017).

In summary, DSC thermograms revealed that lignin laurates exhibited melting behaviors which could be attributed to the van der Waals interaction between the fatty acid substituents. Further work is needed to understand the higher molecular mobility of Dawn lignin after esterification. Nevertheless, these findings suggest that La-Lignins could have suitable applications in adhesives and thermoplastic blends where van der Waals interactions play an important role.

4.2 Preparation of LNPs and La-LNPs

Dawn lignin and its esters were transformed into water-dispersible nanoparticles, which were intended to be used as Pickering stabilizers for oil-in-water emulsions. The fabrication of LNPs was achieved through the solvent exchange method. The concentration of Dawn lignin in the THF:EtOH:H$_2$O solvent system during fractionation was determined to be 0.5 wt %. This solution yielded LNPs with a particle diameter of 89 nm and a polydispersity index (PDI) of 0.14, as shown in Figure 15a. These values were similar to the sizes of LNPs prepared from SKL (LignoBoost™) at the same concentration and solvent system (Lintinen et al., 2018). Furthermore, the LNPs from Dawn lignin had a zeta potential of -47.9 mV, as measured at pH 5.5. This negative surface charge comes from the deprotonated carboxylic groups of the lignin molecules on the particle surface. This measurement aligns with the reported values for zeta potential of LNPs, which typically range from -30 to -60 mV (Lievonen et al., 2016; Sipponen et al., 2017a; Zou et al., 2019).

a)
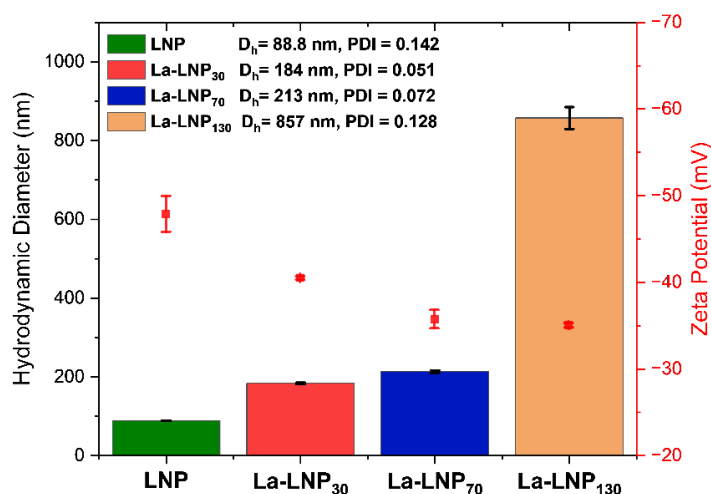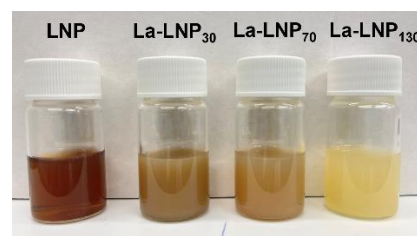
Figure 15. Particle characterization of LNPs and La-LNPs: a) Average particle size and zeta potentials of the lignin particles (LNPs and La-LNPs). b) Digital images of the colloidal dispersions of LNPs and La-LNPs. The error bars in a) represent ± standard deviation from the mean values (n=3).

Similar solvent exchange method was also done to produce La-LNPs. The main difference was that the La-Lignins were dissolved in THF instead of using a solvent system that has a higher relative polarity. As shown in Figure 15b, the color of the dispersion becomes lighter with increasing DS. This could be attributed to the suppression

41

of the free phenolic hydroxyl groups by esterification (Wang et al., 2016). The lighter color of La-LNPs could make them suitable for cosmetic applications.

Colloidal nanoparticles were successfully produced from La-Lignin$_{30}$ which appeared to be a cloudy dispersion (Figure 15b). The particles were almost double in diameter than LNPs from unmodified lignin and exhibited good colloidal stability due to their negative surface charge (-40.5 mV at pH 5.4). After concentration to 0.5 wt% by centrifugation, the particles can be easily redispersed by vortex mixing.

On the other hand, the nanoparticle production for La-Lignin$_{70}$ and La-Lignin$_{130}$ was more challenging. During the solvent exchange process, the esterified lignins strongly aggregated after 15 min of stirring (Appendix B). Hence, the stirring time and speed were decreased which helped prevent the aggregation of La-LNP$_{70}$ resulting to particles with an average diameter of 213 nm. Dialysis was performed for the La-LNPs for organic solvent removal due to issues encountered with rotary evaporation. The rotating motion and heating in rotary evaporator were found to disturb the colloidal dispersion of La-LNP$_{130}$—the particles fused together and stuck into the walls of the flask (Appendix B). This observation led to the speculation that La-LNP$_{130}$ had poor structural integrity which could be traced back to the glue-like property and thermal behavior of La-Lignin$_{130}$. After dialysis, large aggregates of La-LNP$_{70}$ were still observed at the bottom of the membrane. Surprisingly, the average particle sizes for La-LNP$_{130}$ were almost ten times (Ø = 857 nm) the size of the LNPs (Figure 15a).

The attachment of long chain fatty acid affects the overall molecular weight of La-Lignins, as well as their structural motifs. Studies suggest that lignin fractions with smaller molecular weight would form bigger particles due to less hydrophobic interactions (Mattinen et al., 2018). The low M_w of La-LNP$_{30}$ could partially explain its bigger size compared to LNP although the former was expected to have more hydrophobic interactions due to fatty acid substituents. Ideally, smaller average particle diameter should also be observed for La-LNP$_{70}$ and La-LNP$_{130}$ which have higher molecular weights and higher DS, but measurements showed otherwise. Studies on LNPs prepared from esterified lignins show varying observations. Moreno et al. (2021) reported an almost double increase in particle diameter after esterifying SKL with oleic acid prior to solvent exchange, which was in agreement with our findings. Authors attributed this increase to the assembly of oleic acid chains into the core of the particle, though they noted that the degree of substitution does not affect the particle size. In

contrast, tall oil fatty acid esters of SKL produced smaller LNPs compared to its un-modified counterpart (Setälä et al., 2020).

The unexpected large particle sizes of La-LNPs and the thermal instability of La-LNP_{130} dispersions led to further investigations of the morphology of the particles us-ing SEM. The LNPs showed solid spheres uniformly distributed all throughout the substrate (Figure 16a). Interestingly, some spheres had holes or cavities. Similar struc-tures were also observed in La-LNP_{30} (Figure 16b). Single-holed spheres or hollow spheres in LNPs have been previously reported in literature. Li et al. (2021) argued that these holes are a consequence of the drying out of the "hydration zone" formed by the hydrophilic segments of lignin. Xiong et al. (2017) also suggested that the hollow structure is due to the hydrophobic impurities present in THF that cause phase sepa-ration between THF and water during lignin self-assembly. In this case, the type of impurities present would be the wood extractives that were co-extracted during the fractionation step and the residual lauric acid.

Clustering behavior was highly evident in La-LNP_{70} (Figure 16c), which could ex-plain its strong aggregation after dialysis. Unlike La-LNP_{30}, La-LNP_{70} could not be re-dispersed after centrifugation. Aggregation of La-LNPs was most probably due to hy-drophobic interactions of C_{12} chains present on the surface of the particles. Moreno et al. (2021) observed that lignin oleate nanoparticles had core-shells structures with sticky shells and they also attributed this to the oleic chains on particle surfaces.

Figure 16d shows spheres of less than 200 nm attached to the surface of a micron-sized sphere which could point to the possibility that smaller spheres assemble and form bigger particles. This observation could be related to the superstructuring behav-ior of spherical lignin particles as reported in spray-dried LNP dispersions (Lintinen et al., 2018) or evaporation-induced self-assembly of LNPs (B. Zhao et al., 2021).

Lastly, no particles were observed for La-$Lignin_{130}$ as the SEM image shows a mix-ture of round and fused globules instead of discrete, solid spheres (Figure 16e). It seems that, instead of colloidal particle dispersion, a liquid-in-liquid dispersion thus, an emulsion, was observed for La-LNP_{130}. Therefore, it is probable that in the disper-sion state, La-LNP_{130} would coalesce into bigger droplets which could explain the large particle diameter measured by DLS. This is highly likely considering the high molecu-lar mobility of its precursor material wherein DSC findings indicate the onset of melt-ing of La-$Lignin_{130}$ at 10 °C.
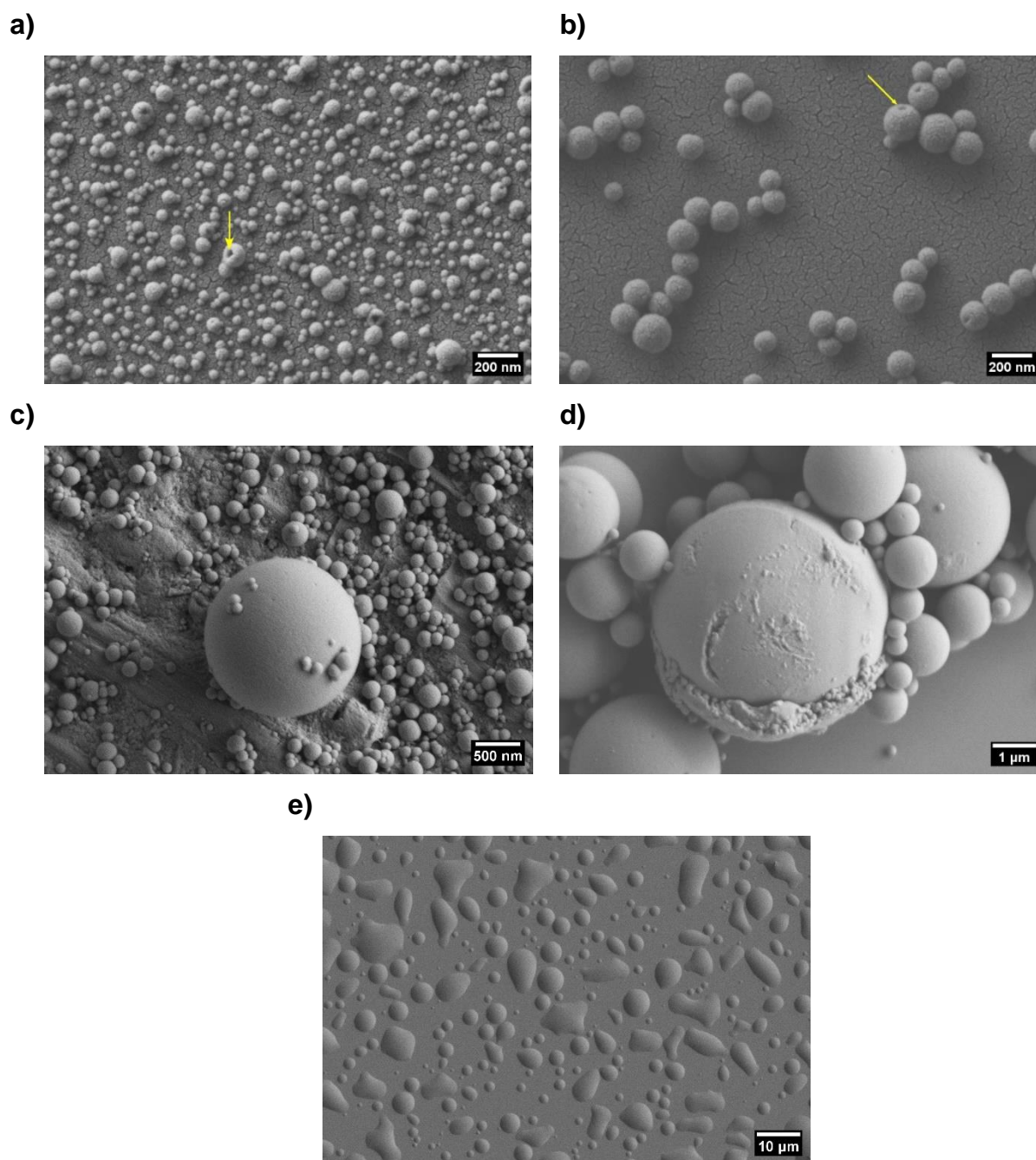
Figure 16. SEM images of the LNPs and La-LNPs: a) LNPs with spheres containing holes (pointed by the yellow arrow). b) La-LNP$_{30}$ also showing some single-holed spheres (pointed by the yellow arrow). c–d) clustering behavior of La-LNP$_{70}$. e) La-LNP$_{130}$ as fused globules.

In summary, the hydrophobic C$_{12}$ fatty acid substituents appear to exert a significant influence on the particle formation or lack thereof of La-LNPs. It is plausible that these substituents would accumulate within the particle resulting to larger spheres. These chains would also be present at the particle surface, similar to the sticky shell structure proposed by Moreno et al. Without enough hydrophilic and charged groups,

the particles can aggregate or fuse together just to avoid contact with water as illustrated in Figure 17. Lastly, the liquid-like behavior exhibited by the precursor La-Lignin$_{130}$ hampers the formation of solid spheres of La-LNP$_{130}$. Further investigations employing advanced microscopic techniques and molecular modeling are warranted to gain deeper insights into the assembly of La-Lignin.
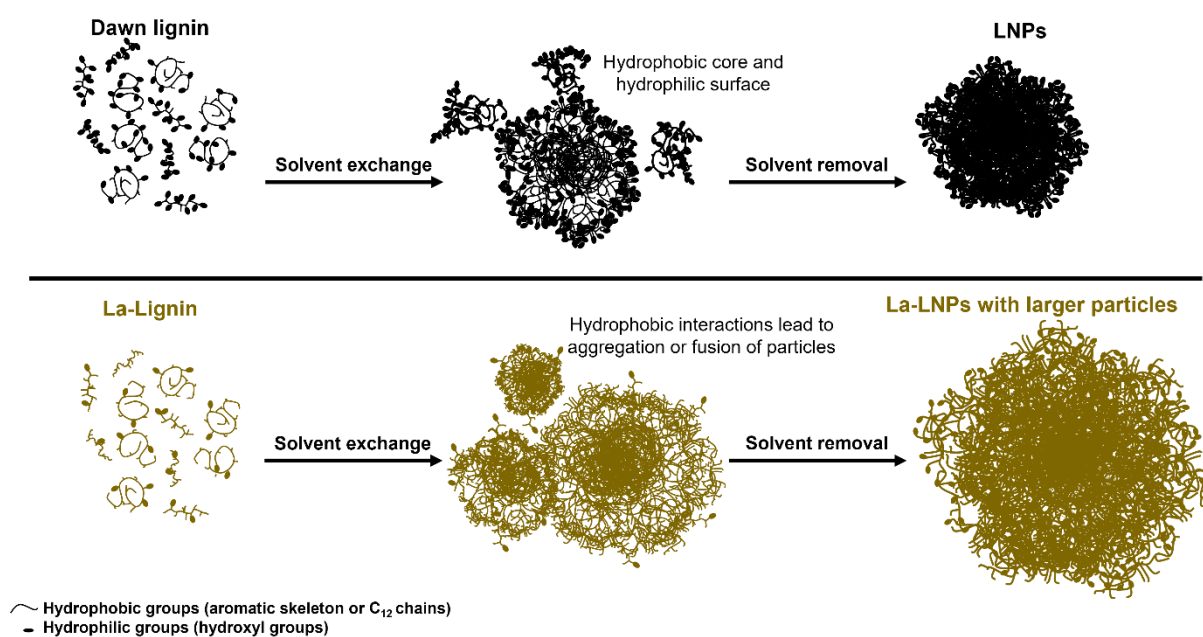
Figure 17. Proposed mechanism for the formation of La-LNPs.

4.3 Performance of LNP and La-LNP as Pickering emulsifiers

The performance of the nanoparticles prepared from Dawn lignin and its esters in stabilizing oil-in-water emulsions was investigated. Olive oil was chosen as the oil phase and the loading of the nanoparticles was held constant at 0.5 wt%. Figure 18a shows that LNP exhibits excellent emulsification performance with the least phase separation among the three emulsion systems. Olive oil seemed to be emulsified as well by La-LNP$_{70}$ because no oil phase separation was visible despite the clear segregation of the aqueous layer. On the other hand, phase separation was highly evident in the emulsion stabilized by La-LNP$_{70}$. The emulsion phase displayed a scattered network of big and heterogeneous droplets.
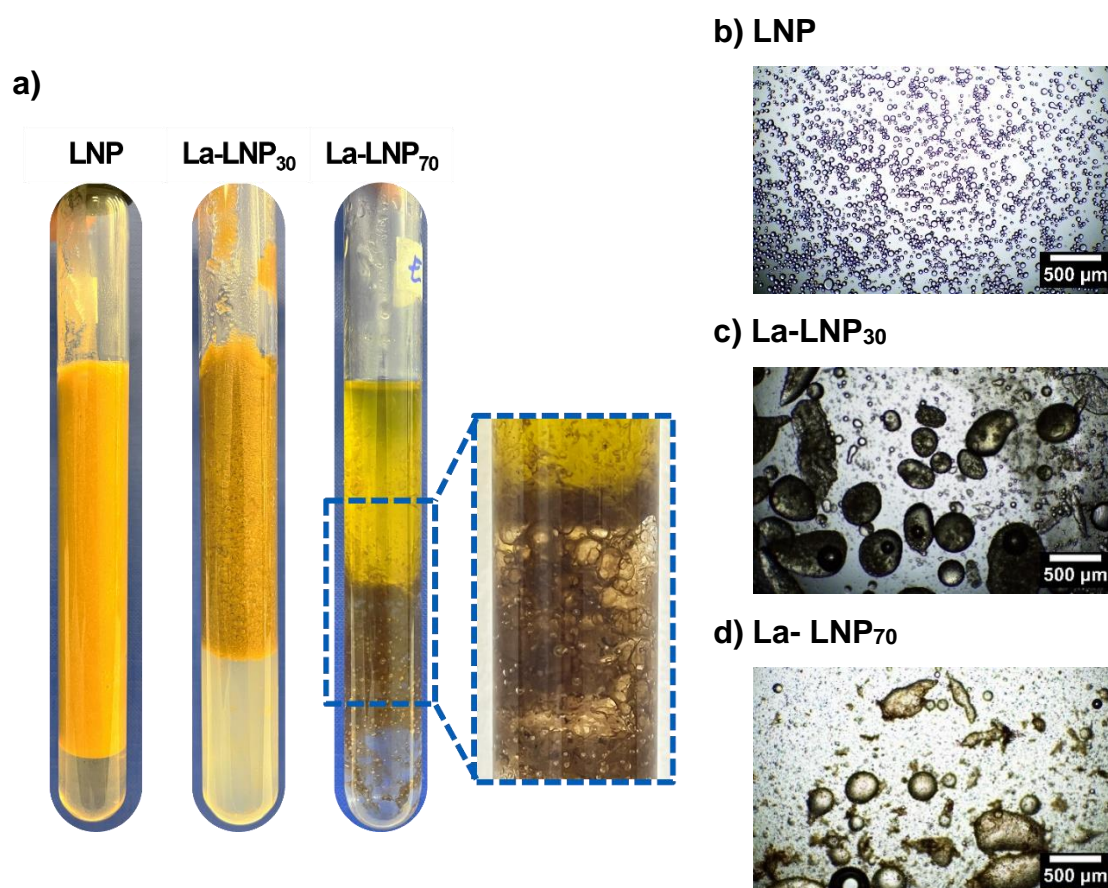
Figure 18. Olive oil-in-water emulsions stabilized by LNP and La-LNPs: a) Visual comparison of the emulsions. Inset shows a zoomed image of the emulsion layer for the La-LNP$_{70}$ system. Micrographs of oil droplets stabilized by b) LNP, c) La-LNP$_{30}$, and d) La-LNP$_{70}$. Images were taken 3 h after preparation of emulsions.

The microstructure of the emulsion phases was observed under an optical microscope. Homogeneous and spherical oil droplets of around 50 μm in diameter were observed for emulsions stabilized by LNP. In comparison, the oil droplets observed

in emulsions stabilized by La-LNP$_{30}$ had bigger sizes ($\leq$ 500 µm is diameter) and heterogeneous geometry. The dark appearance of the droplets suggests that a particle interface was formed around it (Zhang et al., 2019). Lastly, the emulsion stabilized by La-LNP$_{70}$ was difficult to visualize since the droplets had larger diameters than the pipette. The droplets that did not burst showed heterogeneous sizes and geometry.

It was anticipated that La-LNPs would provide better stabilization of olive oil in water than LNPs, given the similar lipophilic structures of lauric acid and triglycerides. However, it appears that other particle properties may have strongly influenced the lower emulsifying capacity of La-LNPs in comparison to LNPs. Previous studies have indicated that smaller particles exhibit higher packing efficiency, resulting in the formation of a more robust interfacial layer and therefore, a more stable Pickering emulsion (Ago et al., 2016; C. Li et al., 2013). Thus, the larger particle sizes of both La-LNP$_{30}$ and La-LNP$_{70}$ could have diminished their effectivity as Pickering emulsifiers compared to LNP. The aggregation of La-LNP$_{70}$ also resulted in their poor dispersibility in the aqueous phase and it increased the effective size of the stabilizing unit, with aggregates adsorbing instead of individual particles (Rayner et al., 2014). Consequently, the emulsification performance of La-LNP$_{70}$ was further compromised.

Since the unmodified LNPs performed surprisingly well, further studies were conducted to investigate the stability of the emulsions. Five emulsions were prepared with varying LNP loading from 0.2 wt% to 2.0 wt%. The volume ratio of olive oil to the LNP dispersion was 1:1 in all five systems. Based on the appearance (Figure 19a), stable Pickering emulsions were already formed at 0.5 wt% with only minimal phase separation. Figure 19b shows that an increase in the loading of the LNPs led to a decrease in the oil droplet diameter, reaching a plateau at 1.5 wt%. The uniformity of the droplet sizes also increased with increasing LNP loading. Moreover, no significant changes in the droplet size and uniformity were observed for emulsions stabilized by 0.5 wt% to 2.0 wt% LNPs and no phase separation occurred even after a month of observation indicating their excellent stability against coalescence.

a)
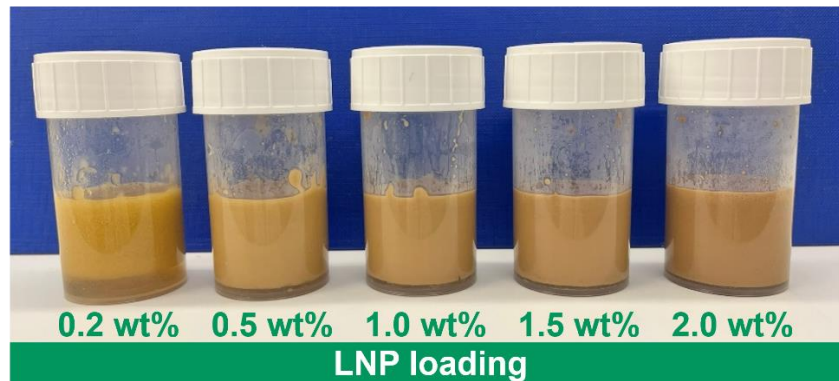
b)
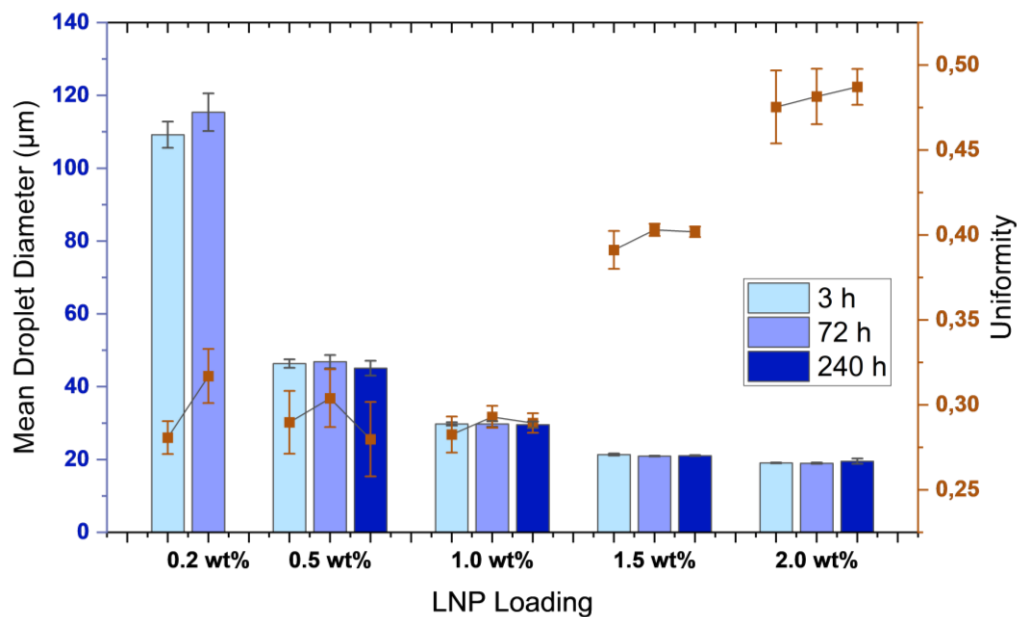
Figure 19. Effect of LNP loading (wt %) on the droplet size of olive oil-in-water emulsions. a) Visual comparison on the emulsions 3 h after preparation. b) Mean droplet diameter and droplet size uniformity as a function of LNP loading. Measurements were done at different time intervals (3, 72, and 240 h). The 240-h data for emulsions stabilized by 0.2 wt% LNP was excluded since there was not enough emulsion layer to measure.

As shown in Figure 20, the oil droplet size is dependent on LNP concentration, and all display spherical geometry. The decrease in droplet size with increasing loading can be explained by the adsorptive kinetics of LNPs. When an adequate number of particles is present to sufficiently cover the oil droplets, an increased particle concentration leads to faster diffusion and adsorption of the particles at the oil-water interface. This results in the formation of smaller and more uniform oil droplets (Ago et al., 2016).
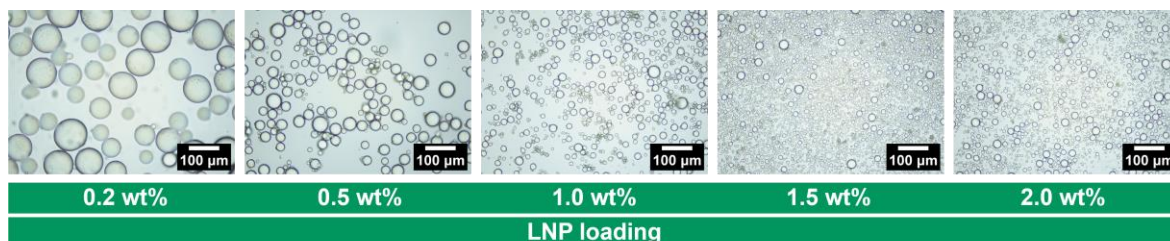
Figure 20. Micrographs of the oil droplets as function of LNP loading taken 3 h after preparation.

Emulsification of triglycerides has been challenging without modifying the surface properties of LNPs. Chemical modification to improve the emulsification properties of LNPs has been done by grafting poly(*N*-isopropylacrylamide onto alkali lignin prior to particle formation (Dai et al., 2019) or by adsorbing cationic polymers (cationic lignin or chitosan) onto LNPs prepared from SKL (Sipponen et al., 2017b; Zou et al., 2019). These studies attributed the improved stability of emulsions to the increased hydrophilicity and cationic charge of the modified LNPs. However, these modifications require additional materials and include more processing steps which could impact its scalability. Findings of this study show that LNPs from Dawn lignin possess sufficient hydrophilic character to stabilize olive oil-in-water emulsions without the need of modifying the lignin precursor. This could open up its applicability in drug delivery where triglycerides are good solvents in lipid-based formulations (Kalepu et al., 2013).

5 Conclusions and perspectives

Development of technologies for transforming biorefinery lignin into value-added products requires a combined effort of understanding its unique chemical structure and evaluating its material properties after certain modifications. In this study, Dawn lignin was esterified with a C_{12} fatty acid chloride at varying molar ratios. The effect of this chemical modification on the structure, thermal properties, and self-assembly of Dawn lignin was evaluated. The main findings of this research, along with suggestions for future studies, are outlined below:

1. The esterification of Dawn lignin with lauroyl chloride significantly affected its structure and physicochemical properties. As the degree of substitution increased, the molecular weight of the lignin increased, while the hydroxyl content decreased due to the incorporation of long-chain substituents into the lignin backbone. This resulted in the reduced hydrophilicity and polarity of the lignin laurates wherein highly substituted lignin esters became more soluble in nonpolar solvents. Moreover, a melting behavior was observed in the esterified lignins. Detailed characterization of the interactions between lignin laurate and other materials would advance its applications in adhesives and polymer blends.

2. The chemical modification of lignin also influenced its particle properties when preparing LNPs. Despite their increased hydrophobic character, larger particles were observed for La-LNPs. Two hypotheses could explain this phenomenon: 1) hydrophobic laurate chains assemble into the core leading to an overall increased size of the particle, and 2) these chains also extend to the particle surface encouraging aggregation with nearby particles to avoid contact with water. At higher degrees of substitution, the particles had increased molecular motion, which could also lead to their fusion into bigger particles, or droplets in La-LNP$_{130}$. These theories could be explored further by imaging the particles in wet state. Molecular modeling could also provide a better understanding of the interactions involved in the self-assembly of La-LNPs.

3. The LNPs from unmodified Dawn lignin demonstrated superior performance in stabilizing olive oil-in-water emulsions compared to La-LNPs. Emulsions were already stable against coalescence with small droplet sizes and high uniformity over a 10-day period at a LNP concentration of 0.5 wt%. Increasing

the LNP concentration further reduced the droplet sizes and improved droplet uniformity. To optimize this process, other variables such as volume fraction, pH, type of oil, and other process parameters can be evaluated using different stability tests. Nevertheless, this emulsion system shows promising potential in food, cosmetics, and biomedical applications where non-toxic materials are of high priority.

References

Ago, M., Huan, S., Borghei, M., Raula, J., Kauppinen, E. I., & Rojas, O. J. (2016). High-Throughput Synthesis of Lignin Particles (~30 nm to ~2 μm) via Aerosol Flow Reactor: Size Fractionation and Utilization in Pickering Emulsions. *ACS Applied Materials & Interfaces*, *8*(35), 23302–23310. https://doi.org/10.1021/acsami.6b07900

Arditty, S., Whitby, C. P., Binks, B. P., Schmitt, V., & Leal-Calderon, F. (2003). Some general features of limited coalescence in solid-stabilized emulsions. *The European Physical Journal E*, *11*(3), 273–281. https://doi.org/10.1140/epje/i2003-10018-6

Asikkala, J., Tamminen, T., & Argyropoulos, D. S. (2012). Accurate and Reproducible Determination of Lignin Molar Mass by Acetobromination. *Journal of Agricultural and Food Chemistry*, *60*(36), 8968–8973. https://doi.org/10.1021/jf303003d

Badmus, S. O., Amusa, H. K., Oyehan, T. A., & Saleh, T. A. (2021). Environmental risks and toxicity of surfactants: Overview of analysis, assessment, and remediation techniques. *Environmental Science and Pollution Research*, *28*(44), 62085–62104. https://doi.org/10.1007/s11356-021-16483-w

Bajwa, D. S., Pourhashem, G., Ullah, A. H., & Bajwa, S. G. (2019). A concise review of current lignin production, applications, products and their environmental impact. *Industrial Crops and Products*, *139*, 111526. https://doi.org/10.1016/j.indcrop.2019.111526

Beckham, G. T., Johnson, C. W., Karp, E. M., Salvachúa, D., & Vardon, D. R. (2016). Opportunities and challenges in biological lignin valorization. *Current Opinion in Biotechnology*, *42*, 40–53. https://doi.org/10.1016/j.copbio.2016.02.030

Bogolitsyn, K. G., Gusakova, M. A., Sloboda, A. A., & Pokryshkin, S. A. (2014). Chemical composition of extractives of normal and rotten aspen (Populus tremula) wood. *Russian Chemical Bulletin*, *63*(9), 2169–2174. https://doi.org/10.1007/s11172-014-0715-3

Börcsök, Z., & Pásztory, Z. (2021). The role of lignin in wood working processes using elevated temperatures: An abbreviated literature survey. *European Journal of Wood and Wood Products*, *79*(3), 511–526. https://doi.org/10.1007/s00107-020-01637-3

Bose, S. K., Francis, R. C., Govender, M., Bush, T., & Spark, A. (2009). Lignin content versus syringyl to guaiacyl ratio amongst poplars. *Bioresource Technology*, *100*(4), 1628–1633. https://doi.org/10.1016/j.biortech.2008.08.046

Constant, S., Wienk, H. L. J., Frissen, A. E., Peinder, P. de, Boelens, R., van Es, D. S., Grisel, R. J. H., Weckhuysen, B. M., Huijgen, W. J. J., Gosselink, R. J. A., & Bruijnincx, P. C. A. (2016). New insights into the structure and composition of technical lignins: A comparative characterisation study. *Green Chemistry*, *18*(9), 2651–2665. https://doi.org/10.1039/C5GC03043A

Dai, L., Li, Y., Kong, F., Liu, K., Si, C., & Ni, Y. (2019). Lignin-Based Nanoparticles Stabilized Pickering Emulsion for Stability Improvement and Thermal-Controlled Release of *trans* -Resveratrol. *ACS Sustainable Chemistry & Engineering*, *7*(15), 13497–13504. https://doi.org/10.1021/acssuschemeng.9b02966

Dessbesell, L., Paleologou, M., Leitch, M., Pulkki, R., & Xu, C. (Charles). (2020). Global lignin supply overview and kraft lignin potential as an alternative for

petroleum-based polymers. *Renewable and Sustainable Energy Reviews*, *123*, 109768. https://doi.org/10.1016/j.rser.2020.109768

Doherty, W. O. S., Mousavioun, P., & Fellows, C. M. (2011). Value-adding to cellulosic ethanol: Lignin polymers. *Industrial Crops and Products*, *33*(2), 259–276. https://doi.org/10.1016/j.indcrop.2010.10.022

Duval, A., & Lawoko, M. (2014). A review on lignin-based polymeric, micro- and nano-structured materials. *Reactive and Functional Polymers*, *85*, 78–96. https://doi.org/10.1016/j.reactfunctpolym.2014.09.017

Ekielski, A., & Mishra, P. K. (2020). Lignin for Bioeconomy: The Present and Future Role of Technical Lignin. *International Journal of Molecular Sciences*, *22*(1), 63. https://doi.org/10.3390/ijms22010063

Farooq, M., Zou, T., Valle-Delgado, J. J., Sipponen, M. H., Morits, M., & Österberg, M. (2020). Well-Defined Lignin Model Films from Colloidal Lignin Particles. *Langmuir*, *36*(51), 15592–15602. https://doi.org/10.1021/acs.langmuir.0c02970

Fengel, D., & Wegener, G. (2011). *Wood: Chemistry, ultrastructure, reactions*. De Gruyter.

Fernández-Rodríguez, J., Erdocia, X., Sánchez, C., González Alriols, M., & Labidi, J. (2017). Lignin depolymerization for phenolic monomers production by sustainable processes. *Journal of Energy Chemistry*, *26*(4), 622–631. https://doi.org/10.1016/j.jechem.2017.02.007

Figueiredo, P., Lintinen, K., Hirvonen, J. T., Kostiainen, M. A., & Santos, H. A. (2018). Properties and chemical modifications of lignin: Towards lignin-based nanomaterials for biomedical applications. *Progress in Materials Science*, *93*, 233–269. https://doi.org/10.1016/j.pmatsci.2017.12.001

Fox, S. C., Li, B., Xu, D., & Edgar, K. J. (2011). Regioselective Esterification and Etherification of Cellulose: A Review. *Biomacromolecules*, *12*(6), 1956–1972. https://doi.org/10.1021/bm200260d

Ge, Y., & Li, Z. (2018). Application of Lignin and Its Derivatives in Adsorption of Heavy Metal Ions in Water: A Review. *ACS Sustainable Chemistry & Engineering*, *6*(5), 7181–7192. https://doi.org/10.1021/acssuschemeng.8b01345

Gierer, J. (1980). Chemical aspects of kraft pulping. *Wood Science and Technology*, *14*(4), 241–266. https://doi.org/10.1007/BF00383453

Gordobil, O., Blažević, N., Simonič, M., & Sandak, A. (2023). Potential of lignin multifunctionality for a sustainable skincare: Impact of emulsification process parameters and oil-phase on the characteristics of O/W Pickering emulsions. *International Journal of Biological Macromolecules*, *233*, 123561. https://doi.org/10.1016/j.ijbiomac.2023.123561

Guo, Z.-X., Gandini, A., & Pla, F. (1992). Polyesters from lignin. 1. The reaction of kraft lignin with dicarboxylic acid chlorides. *Polymer International*, *27*(1), 17–22. https://doi.org/10.1002/pi.4990270104

Hedenström, M., Wiklund-Lindström, S., Öman, T., Lu, F., Gerber, L., Schatz, P., Sundberg, B., & Ralph, J. (2009). Identification of Lignin and Polysaccharide Modifications in Populus Wood by Chemometric Analysis of 2D NMR Spectra from Dissolved Cell Walls. *Molecular Plant*, *2*(5), 933–942. https://doi.org/10.1093/mp/ssp047

Hua, Q., Liu, L.-Y., Karaaslan, M. A., & Renneckar, S. (2019). Aqueous Dispersions of Esterified Lignin Particles for Hydrophobic Coatings. *Frontiers in Chemistry*, *7*, 515. https://doi.org/10.3389/fchem.2019.00515

Huang, J., Wang, M., Song, P., Li, Y., Xu, F., & Zhang, X. (2019). Directed 2D nanosheet assemblies of amphiphilic lignin derivatives: Formation of hollow spheres with tunable porous structure. *Industrial Crops and Products*, *127*, 16–25. https://doi.org/10.1016/j.indcrop.2018.10.036

Hult, E.-L., Koivu, K., Asikkala, J., Ropponen, J., Wrigstedt, P., Sipilä, J., & Poppius-Levlin, K. (2013). Esterified lignin coating as water vapor and oxygen barrier for fiber-based packaging. *Hfsg*, *67*(8), 899–905. https://doi.org/10.1515/hf-2012-0214

Kadla, J. F., Kubo, S., Venditti, R. A., Gilbert, R. D., Compere, A. L., & Griffith, W. (2002). Lignin-based carbon fibers for composite fiber applications. *Carbon*, *40*(15), 2913–2920. https://doi.org/10.1016/S0008-6223(02)00248-8

Kalepu, S., Manthina, M., & Padavala, V. (2013). Oral lipid-based drug delivery systems – an overview. *Acta Pharmaceutica Sinica B*, *3*(6), 361–372. https://doi.org/10.1016/j.apsb.2013.10.001

Kimiaei, E., Farooq, M., Grande, R., Meinander, K., & Österberg, M. (2022). Lignin Nanoparticles as an Interfacial Modulator in Tough and Multi-Resistant Cellulose–Polycaprolactone Nanocomposites Based on a Pickering Emulsions Strategy. *Advanced Materials Interfaces*, *9*(27), 2200988. https://doi.org/10.1002/admi.202200988

Koivu, K. A. Y., Sadeghifar, H., Nousiainen, P. A., Argyropoulos, D. S., & Sipilä, J. (2016). Effect of Fatty Acid Esterification on the Thermal Properties of Softwood Kraft Lignin. *ACS Sustainable Chemistry & Engineering*, *4*(10), 5238–5247. https://doi.org/10.1021/acssuschemeng.6b01048

Kralchevsky, P. A., Ivanov, I. B., Ananthapadmanabhan, K. P., & Lips, A. (2005). On the Thermodynamics of Particle-Stabilized Emulsions: Curvature Effects and Catastrophic Phase Inversion. *Langmuir*, *21*(1), 50–63. https://doi.org/10.1021/la047793d

Laurichesse, S., & Avérous, L. (2014). Chemical modification of lignins: Towards biobased polymers. *Progress in Polymer Science*, *39*(7), 1266–1290. https://doi.org/10.1016/j.progpolymsci.2013.11.004

Leskinen, T., Smyth, M., Xiao, Y., Lintinen, K., Mattinen, M.-L., Kostiainen, M. A., Oinas, P., & Österberg, M. (2017). Scaling Up Production of Colloidal Lignin Particles. *Nordic Pulp & Paper Research Journal*, *32*(4), 586–596. https://doi.org/10.3183/npprj-2017-32-04_p586-596_leskinen

Leskinen, T., Witos, J., Valle-Delgado, J. J., Lintinen, K., Kostiainen, M., Wiedmer, S. K., Österberg, M., & Mattinen, M.-L. (2017). Adsorption of Proteins on Colloidal Lignin Particles for Advanced Biomaterials. *Biomacromolecules*, *18*(9), 2767–2776. https://doi.org/10.1021/acs.biomac.7b00676

Li, B., You, S., Qi, W., Wang, Y., Su, R., & He, Z. (2020). Structure-tunable assembly of lignin sub-micro spheres by modifying the amphiphilic interfaces of lignin via n-alkane. *European Polymer Journal*, *126*, 109539. https://doi.org/10.1016/j.eurpolymj.2020.109539

Li, C., Li, Y., Sun, P., & Yang, C. (2013). Pickering emulsions stabilized by native starch granules. *Colloids and Surfaces A: Physicochemical and Engineering Aspects*, *431*, 142–149. https://doi.org/10.1016/j.colsurfa.2013.04.025

Li, C., Zhao, X., Wang, A., Huber, G. W., & Zhang, T. (2015). Catalytic Transformation of Lignin for the Production of Chemicals and Fuels. *Chemical Reviews*, *115*(21), 11559–11624. https://doi.org/10.1021/acs.chemrev.5b00155

Li, S., Zhou, S., & Zhao, G. (2021). Tuning the morphology of micro- and nano-spheres from bamboo shoot shell acetosolv lignin. *Industrial Crops and Products*, *171*, 113860. https://doi.org/10.1016/j.indcrop.2021.113860

Li, W., Jiao, B., Li, S., Faisal, S., Shi, A., Fu, W., Chen, Y., & Wang, Q. (2022). Recent Advances on Pickering Emulsions Stabilized by Diverse Edible Particles: Stability Mechanism and Applications. *Frontiers in Nutrition*, *9*, 864943. https://doi.org/10.3389/fnut.2022.864943

Lievonen, M., Valle-Delgado, J. J., Mattinen, M.-L., Hult, E.-L., Lintinen, K., Kostiainen, M. A., Paananen, A., Szilvay, G. R., Setälä, H., & Österberg, M. (2016). A simple process for lignin nanoparticle preparation. *Green Chemistry*, *18*(5), 1416–1422. https://doi.org/10.1039/C5GC01436K

Lintinen, K., Xiao, Y., Bangalore Ashok, R., Leskinen, T., Sakarinen, E., Sipponen, M., Muhammad, F., Oinas, P., Österberg, M., & Kostiainen, M. (2018). Closed cycle production of concentrated and dry redispersible colloidal lignin particles with a three solvent polarity exchange method. *Green Chemistry*, *20*(4), 843–850. https://doi.org/10.1039/C7GC03465B

Luo, S., Cao, J., & McDonald, A. G. (2017). Esterification of industrial lignin and its effect on the resulting poly(3-hydroxybutyrate-co-3-hydroxyvalerate) or polypropylene blends. *Industrial Crops and Products*, *97*, 281–291. https://doi.org/10.1016/j.indcrop.2016.12.024

Marchand, G., Fabre, G., Maldonado-Carmona, N., Villandier, N., & Leroy-Lhez, S. (2020). Acetylated lignin nanoparticles as a possible vehicle for photosensitizing molecules. *Nanoscale Advances*, *2*(12), 5648–5658. https://doi.org/10.1039/D0NA00615G

Mattinen, M.-L., Riviere, G., Henn, A., Nugroho, R., Leskinen, T., Nivala, O., Valle-Delgado, J., Kostiainen, M., & Österberg, M. (2018). Colloidal Lignin Particles as Adhesives for Soft Materials. *Nanomaterials*, *8*(12), 1001. https://doi.org/10.3390/nano8121001

Meng, X., Crestini, C., Ben, H., Hao, N., Pu, Y., Ragauskas, A. J., & Argyropoulos, D. S. (2019). Determination of hydroxyl groups in biorefinery resources via quantitative 31P NMR spectroscopy. *Nature Protocols*, *14*(9), 2627–2647. https://doi.org/10.1038/s41596-019-0191-1

Moreno, A., Liu, J., Gueret, R., Hadi, S. E., Bergström, L., Slabon, A., & Sipponen, M. H. (2021). Unravelling the Hydration Barrier of Lignin Oleate Nanoparticles for Acid- and Base-Catalyzed Functionalization in Dispersion State. *Angewandte Chemie International Edition*, *60*(38), 20897–20905. https://doi.org/10.1002/anie.202106743

Nadji, H., Rodrigue, D., Benaboura, A., Bédard, Y., Stevanovic, T., & Riedl, B. (2009). Value-added derivatives of soda lignin Alfa grass (*Stipa tenacissima*). II. Uses as lubricants in plastic processing. *Journal of Applied Polymer Science*, *114*(5), 3003–3007. https://doi.org/10.1002/app.30925

Österberg, M., Henn, K. A., Farooq, M., & Valle-Delgado, J. J. (2023). Biobased Nanomaterials—The Role of Interfacial Interactions for Advanced Materials. *Chemical Reviews*, acs.chemrev.2c00492. https://doi.org/10.1021/acs.chemrev.2c00492

Österberg, M., Sipponen, M. H., Mattos, B. D., & Rojas, O. J. (2020). Spherical lignin particles: A review on their sustainability and applications. *Green Chemistry*, *22*(9), 2712–2733. https://doi.org/10.1039/D0GC00096E

Pawar, S. N., Venditti, R. A., Jameel, H., Chang, H.-M., & Ayoub, A. (2016). Engineering physical and chemical properties of softwood kraft lignin by fatty acid

substitution. *Industrial Crops and Products*, *89*, 128–134. https://doi.org/10.1016/j.indcrop.2016.04.070

Portes Abraham Silva, Y. (2022). *Biorefinery lignin: Structural characterization, modification and production of nanoparticles for applications* [Aalto University]. http://urn.fi/URN:NBN:fi:aalto-202208305234

Pylypchuk, I. V., Karlsson, M., Lindén, P. A., Lindström, M. E., Elder, T., Sevastyanova, O., & Lawoko, M. (2023). Molecular understanding of the morphology and properties of lignin nanoparticles: Unravelling the potential for tailored applications. *Green Chemistry*, 10.1039.D3GC00703K. https://doi.org/10.1039/D3GC00703K

Qian, Y., Deng, Y., Qiu, X., Li, H., & Yang, D. (2014). Formation of uniform colloidal spheres from lignin, a renewable resource recovered from pulping spent liquor. *Green Chemistry*, *16*(4), 2156. https://doi.org/10.1039/c3gc42131g

Ragauskas, A. J., Beckham, G. T., Biddy, M. J., Chandra, R., Chen, F., Davis, M. F., Davison, B. H., Dixon, R. A., Gilna, P., Keller, M., Langan, P., Naskar, A. K., Saddler, J. N., Tschaplinski, T. J., Tuskan, G. A., & Wyman, C. E. (2014). Lignin Valorization: Improving Lignin Processing in the Biorefinery. *Science*, *344*(6185), 1246843. https://doi.org/10.1126/science.1246843

Ralph, J., & Landucci, L. (2010). NMR of Lignins. In C. Heitner, D. Dimmel, & J. Schmidt (Eds.), *Lignin and Lignans* (pp. 137–243). CRC Press. https://doi.org/10.1201/EBK1574444865-c5

Ralph, J., Lapierre, C., & Boerjan, W. (2019). Lignin structure and its engineering. *Current Opinion in Biotechnology*, *56*, 240–249. https://doi.org/10.1016/j.copbio.2019.02.019

Ralph, J., Lundquist, K., Brunow, G., Lu, F., Kim, H., Schatz, P. F., Marita, J. M., Hatfield, R. D., Ralph, S. A., Christensen, J. H., & Boerjan, W. (2004). Lignins: Natural polymers from oxidative coupling of 4-hydroxyphenyl- propanoids. *Phytochemistry Reviews*, *3*(1–2), 29–60. https://doi.org/10.1023/B:PHYT.0000047809.65444.a4

Rayner, M., Marku, D., Eriksson, M., Sjöö, M., Dejmek, P., & Wahlgren, M. (2014). Biomass-based particles for the formulation of Pickering type emulsions in food and topical applications. *Colloids and Surfaces A: Physicochemical and Engineering Aspects*, *458*, 48–62. https://doi.org/10.1016/j.colsurfa.2014.03.053

Schneider, W. D. H., Dillon, A. J. P., & Camassola, M. (2021). Lignin nanoparticles enter the scene: A promising versatile green tool for multiple applications. *Biotechnology Advances*, *47*, 107685. https://doi.org/10.1016/j.biotechadv.2020.107685

Schutyser, W., Renders, T., Van den Bosch, S., Koelewijn, S.-F., Beckham, G. T., & Sels, B. F. (2018). Chemicals from lignin: An interplay of lignocellulose fractionation, depolymerisation, and upgrading. *Chemical Society Reviews*, *47*(3), 852–908. https://doi.org/10.1039/C7CS00566K

Setälä, H., Alakomi, H.-L., Paananen, A., Szilvay, G. R., Kellock, M., Lievonen, M., Liljeström, V., Hult, E.-L., Lintinen, K., Österberg, M., & Kostiainen, M. (2020). Lignin nanoparticles modified with tall oil fatty acid for cellulose functionalization. *Cellulose*, *27*(1), 273–284. https://doi.org/10.1007/s10570-019-02771-9

Sharma, A., Kaur, P., Singh, G., & Arya, S. K. (2021). Economical concerns of lignin in the energy sector. *Cleaner Engineering and Technology*, *4*, 100258. https://doi.org/10.1016/j.clet.2021.100258

Sipponen, M. H., Lange, H., Ago, M., & Crestini, C. (2018). Understanding Lignin Aggregation Processes. A Case Study: Budesonide Entrapment and Stimuli Controlled Release from Lignin Nanoparticles. *ACS Sustainable Chemistry & Engineering*, *6*(7), 9342–9351. https://doi.org/10.1021/acssuschemeng.8b01652

Sipponen, M. H., Smyth, M., Leskinen, T., Johansson, L.-S., & Österberg, M. (2017a). All-lignin approach to prepare cationic colloidal lignin particles: Stabilization of durable Pickering emulsions. *Green Chemistry*, *19*(24), 5831–5840. https://doi.org/10.1039/C7GC02900D

Sipponen, M. H., Smyth, M., Leskinen, T., Johansson, L.-S., & Österberg, M. (2017b). All-lignin approach to prepare cationic colloidal lignin particles: Stabilization of durable Pickering emulsions. *Green Chemistry*, *19*(24), 5831–5840. https://doi.org/10.1039/C7GC02900D

Siram, K., Habibur Rahman, S. M., Balakumar, K., Duganath, N., Chandrasekar, R., & Hariprasad, R. (2019). Pharmaceutical nanotechnology: Brief perspective on lipid drug delivery and its current scenario. In *Biomedical Applications of Nanoparticles* (pp. 91–115). Elsevier. https://doi.org/10.1016/B978-0-12-816506-5.00005-X

Tarasov, D., Schlee, P., Pranovich, A., Moreno, A., Wang, L., Rigo, D., Sipponen, M. H., Xu, C., & Balakshin, M. (2022). AqSO biorefinery: A green and parameter-controlled process for the production of lignin–carbohydrate hybrid materials. *Green Chemistry*, *24*(17), 6639–6656. https://doi.org/10.1039/D2GC02171D

Thielemans, W., & Wool, R. P. (2005). Lignin Esters for Use in Unsaturated Thermosets: Lignin Modification and Solubility Modeling. *Biomacromolecules*, *6*(4), 1895–1905. https://doi.org/10.1021/bm0500345

Tian, D., Hu, J., Chandra, R. P., Saddler, J. N., & Lu, C. (2017). Valorizing Recalcitrant Cellulolytic Enzyme Lignin via Lignin Nanoparticles Fabrication in an Integrated Biorefinery. *ACS Sustainable Chemistry & Engineering*, *5*(3), 2702–2710. https://doi.org/10.1021/acssuschemeng.6b03043

Tomasich, J., Beisl, S., & Harasek, M. (2023). Production and Characterisation of Pickering Emulsions Stabilised by Colloidal Lignin Particles Produced from Various Bulk Lignins. *Sustainability*, *15*(4), 3693. https://doi.org/10.3390/su15043693

Van den Bosch, S., Koelewijn, S.-F., Renders, T., Van den Bossche, G., Vangeel, T., Schutyser, W., & Sels, B. F. (2018). Catalytic Strategies Towards Lignin-Derived Chemicals. *Topics in Current Chemistry*, *376*(5), 36. https://doi.org/10.1007/s41061-018-0214-3

Van Putten, R.-J., Mckay, B., Gruter, G. J. M., & Van der Waal, J. C. (2019). *A process for the conversion of a solid lignocellulosic material* (Patent No. WO 2019/149853 A1).

Wang, F. (2022). *Supramolecular colloidal assembly of flow hydrolysis hardwood lignin from Dawn technology™ process* [Aalto University]. http://urn.fi/URN:NBN:fi:aalto-202205223308

Wang, J., Deng, Y., Qian, Y., Qiu, X., Ren, Y., & Yang, D. (2016). Reduction of lignin color via one-step UV irradiation. *Green Chemistry*, *18*(3), 695–699. https://doi.org/10.1039/C5GC02180D

Wen, X., Wang, H., Wei, Y., Wang, X., & Liu, C. (2017). Preparation and characterization of cellulose laurate ester by catalyzed transesterification.

Carbohydrate Polymers, *168*, 247–254. https://doi.org/10.1016/j.carbpol.2017.03.074

Xiong, F., Han, Y., Wang, S., Li, G., Qin, T., Chen, Y., & Chu, F. (2017). Preparation and Formation Mechanism of Renewable Lignin Hollow Nanospheres with a Single Hole by Self-Assembly. *ACS Sustainable Chemistry & Engineering*, *5*(3), 2273–2281. https://doi.org/10.1021/acssuschemeng.6b02585

Xu, C. C., Dessbesell, L., Zhang, Y., & Yuan, Z. (2021). Lignin valorization beyond energy use: Has lignin's time finally come? *Biofuels, Bioproducts and Biorefining*, *15*(1), 32–36. https://doi.org/10.1002/bbb.2172

Zhang, L., Lei, Q., Luo, J., Zeng, M., Wang, L., Huang, D., Wang, X., Mannan, S., Peng, B., & Cheng, Z. (2019). Natural Halloysites-Based Janus Platelet Surfactants for the Formation of Pickering Emulsion and Enhanced Oil Recovery. *Scientific Reports*, *9*(1), 163. https://doi.org/10.1038/s41598-018-36352-w

Zhao, B., Borghei, M., Zou, T., Wang, L., Johansson, L.-S., Majoinen, J., Sipponen, M. H., Österberg, M., Mattos, B. D., & Rojas, O. J. (2021). Lignin-Based Porous Supraparticles for Carbon Capture. *ACS Nano*, *15*(4), 6774–6786. https://doi.org/10.1021/acsnano.0c10307

Zhao, X., Zhang, Y., Wei, L., Hu, H., Huang, Z., Yang, M., Huang, A., Wu, J., & Feng, Z. (2017). Esterification mechanism of lignin with different catalysts based on lignin model compounds by mechanical activation-assisted solid-phase synthesis. *RSC Advances*, *7*(83), 52382–52390. https://doi.org/10.1039/C7RA10482K

Zou, T., Sipponen, M. H., & Österberg, M. (2019). Natural Shape-Retaining Microcapsules With Shells Made of Chitosan-Coated Colloidal Lignin Particles. *Frontiers in Chemistry*, *7*, 370. https://doi.org/10.3389/fchem.2019.00370

Appendix

a)

b)

c)

Appendix A. Appearance of esterified lignins: a) La-Lignin$_{30}$, b) La-Lignin$_{70}$, and c) La-Lignin$_{130}$ as thick, oily material.

a)

b)

Appendix B. Issues encountered during La-LNP production: a) Aggregation and phase separation of La-LNP$_{70}$. b) La-LNP$_{130}$ stuck into the walls of the round bottom flask during rotary evaporation.